ANL/ESD-16/10

Systematic Evaluation of Stochastic Methods in Power System Scheduling and Dispatch with Renewable Energy

Energy Systems Division

About Argonne National Laboratory
Argonne is a U.S. Department of Energy laboratory managed by UChicago Argonne, LLC under contract DE-AC02-06CH11357. The Laboratory's main facility is outside Chicago, at 9700 South Cass Avenue, Argonne, Illinois 60439. For information about Argonne and its pioneering science and technology programs, see www.anl.gov.

DOCUMENT AVAILABILITY

Online Access: U.S. Department of Energy (DOE) reports produced after 1991 and a growing number of pre-1991 documents are available free via DOE's SciTech Connect (http://www.osti.gov/scitech/).

Reports not in digital format may be purchased by the public from the National Technical Information Service (NTIS):
U.S. Department of Commerce
National Technical Information Service
5301 Shawnee Rd
Alexandria, VA 22312
www.ntis.gov
Phone: (800) 553-NTIS (6847) or (703) 605-6000
Fax: (703) 605-6900
Email: **orders@ntis.gov**

Reports not in digital format are available to DOE and DOE contractors from the Office of Scientific and Technical Information (OSTI):
U.S. Department of Energy
Office of Scientific and Technical Information
P.O. Box 62
Oak Ridge, TN 37831-0062
www.osti.gov
Phone: (865) 576-8401
Fax: (865) 576-5728
Email: **reports@osti.gov**

Disclaimer
This report was prepared as an account of work sponsored by an agency of the United States Government. Neither the United States Government nor any agency thereof, nor UChicago Argonne, LLC, nor any of their employees or officers, makes any warranty, express or implied, or assumes any legal liability or responsibility for the accuracy, completeness, or usefulness of any information, apparatus, product, or process disclosed, or represents that its use would not infringe privately owned rights. Reference herein to any specific commercial product, process, or service by trade name, trademark, manufacturer, or otherwise, does not necessarily constitute or imply its endorsement, recommendation, or favoring by the United States Government or any agency thereof. The views and opinions of document authors expressed herein do not necessarily state or reflect those of the United States Government or any agency thereof, Argonne National Laboratory, or UChicago Argonne, LLC.

ANL/ESD-16/10

Systematic Evaluation of Stochastic Methods in Power System Scheduling and Dispatch with Renewable Energy

by
Yishen Wang,[1,2] Zhi Zhou,[2] Cong Liu,[2,3] and Audun Botterud[2]
[1]University of Washington
[2]Argonne National Laboratory
[3]Electric Reliability Council of Texas (ERCOT)

August 2016

CONTENTS

ACKNOWLEDGMENT v
SUMMARY 1
1 INTRODUCTION 2
2 WIND POWER PROBABILISTIC FORECASTING AND REPRESENTATION 4
2.1 Probabilistic Forecasting 4
2.2 Scenario Generation with Spatio-temporal Correlation 4
2.2 Scenario Reduction 5
3 METHODS AND FORMULATIONS 7
3.1 Nomenclature 7
3.2 Deterministic Formulation with Dynamic Reserve Strategies 10
3.3 Stochastic Programming-based Formulation 15
3.4 Stochastic Programming Formulation with Decomposition Methods 15
3.4.1 Linear-Shift-Factor Decomposition 16
3.4.2 Benders Decomposition 16
3.5 Interval Optimization-based Formulation 20
4 TEST SYSTEM AND DATA 22
4.1 IEEE 118-bus System 22
4.2 Load Demand and Generation Supply 22
4.3 Transmission Network 23
4.4 Zonal Setting 23
4.5 Wind Farm Deployment 23
4.6 Decision Framework 24
4.7 Simulation Settings 25
5 RESULTS AND ANALYSIS 26
5.1 Case Study Description 26
5.2 Production Cost 26
5.2.1 Day-ahead Costs 26
5.2.2 Real-time Costs 31
5.3 Reserve Costs 33
5.4 Curtailment of Reserve and Load 33
5.4.1 Day-ahead 33
5.4.2 Real-time 38
5.5 Wind Curtailment 39
5.6 Number of Commitments 39
5.7 Computation 41
6 CONCLUSION AND FUTURE DIRECTIONS 44
7 REFERENCES 46

FIGURES

1 Reduced Scenarios and Confidence Interval for Wind Power 6
2 IEEE-118 System One-line Diagram..... 22
3 Decision-making Processes 24

TABLES

1 IEEE 118 Zonal Information 23
2 Case Description. All cases use a 21% available wind penetration 27
3 Summer Average Daily Day-ahead Total Cost 28
4 Summer Average Daily Day-ahead Total Energy Cost..... 29
5 Fall Average Daily Day-ahead Total Cost..... 29
6 Fall Average Daily Day-ahead Energy Cost 30
7 Summer Average Daily Real-time Total Cost..... 32
8 Fall Average Daily Real-time Total Cost 32
9 Summer Average Daily Day-ahead Reserve Cost..... 34
10 Fall Average Daily Day-ahead Reserve Cost 34
11 Summer Daily Average Day-ahead Load Shedding Amount..... 35
12 Fall Daily Average Day-ahead Load Shedding Amount..... 35
13 Summer Average Daily Day-ahead Reserve Curtailment..... 36
14 Fall Average Daily Day-ahead Reserve Curtailment 37
15 Four-Month Average Daily Day-ahead Reserve Curtailment for DUC Cases..... 37
16 Fall Average Daily Real-time Load Shedding..... 38
17 Average Daily Total Real-time Wind Curtailments 39
18 Average Daily Number of Commitments..... 40
19 Average Day-ahead Computational Time Per Day 42
20 Average RAC Computational Time Per Day 42
21 LSF Decomposition Convergence Statistics 43
22 Benders Decomposition Convergence Statistics 43
23 Pros and Cons of Different Scheduling Strategies 45

ACKNOWLEDGMENT

This work was supported by the U.S. Department of Energy, Office of Energy Efficiency and Renewable Energy through its Wind and Water Power Program. The submitted manuscript has been created by UChicago Argonne, LLC, Operator of Argonne National Laboratory ("Argonne"). Argonne, a U.S. Department of Energy Office of Science laboratory, is operated under Contract No. DE-AC02–06CH11357.

SUMMARY

As more wind power and other renewable resources are being integrated into the electric power grid, the forecast uncertainty brings operational challenges for the power system operators. In this report, different operational strategies for uncertainty management are presented and evaluated. A comprehensive and consistent simulation framework is developed to analyze the performance of different reserve policies and scheduling techniques under uncertainty in wind power. Numerical simulations are conducted on a modified version of the IEEE 118-bus system with a 20% wind penetration level, comparing deterministic, interval, and stochastic unit commitment strategies. The results show that stochastic unit commitment provides a reliable schedule without large increases in operational costs. Moreover, decomposition techniques, such as load shift factor and Benders decomposition, can help in overcoming the computational obstacles to stochastic unit commitment and enable the use of a larger scenario set to represent forecast uncertainty. In contrast, deterministic and interval unit commitment tend to give higher system costs as more reserves are being scheduled to address forecast uncertainty. However, these approaches require a much lower computational effort Choosing a proper lower bound for the forecast uncertainty is important for balancing reliability and system operational cost in deterministic and interval unit commitment. Finally, we find that the introduction of zonal reserve requirements improves reliability, but at the expense of higher operational costs.

1 INTRODUCTION

The rapidly growing penetration of renewable energy resources has created significant challenges for the electricity markets and grid operators because of their inherent variability and uncertainty. Commonly adopted approaches to address these challenges include advanced forecasting techniques [1]-[7] and improved system operational uncertainty modeling [8]-[25]. Traditionally, the system operators make the commitment and dispatch decisions on the basis of a deterministic renewable point forecast. Numerous statistical methods and machine learning techniques have been applied to the accuracy of wind power forecasting [1]-[7], including Gaussian processes, support vector machines, artificial neural networks, random forest, and others [1]. Although these methods produce a point forecast with improved accuracy, additional information about the uncertainty in the forecast is needed. Recently, probabilistic wind power forecasting has attracted substantial attention as a means to provide wind power's probability distribution in addition to the central point forecast [2]. Kernel density estimation [3], quantile regression, and other parametric or non-parametric algorithms [1]-[2] have been proposed in this context. With such probabilistic information, wind power scenarios or uncertainty sets with a certain confidence level can be properly constructed to feed power system operational models for improved representation of wind power forecast uncertainty.

In the literature, many researchers have applied different operational schemes to incorporate stochastic wind power generation [8]-[25]. These approaches mainly include deterministic unit commitment (DUC) with dynamic reserves [8]-[9], scenario-based stochastic UC (SUC) [8]-[15], interval-based UC (IUC) [16]-[18], robust UC (RUC) [19]-[20], chance-constrained UC [21], and hybrid and unified approaches [22]-[23]. The traditional DUC typically keeps contingency reserves to address the possibility of a generation or line outage. To better account for the stochastic system conditions, including forecast uncertainty, more dynamic operating reserve strategies can be used. For instance, Zhou et al. [8] propose that the dynamic reserve amount be determined through the difference between a central point forecast and a lower-level quantile obtained from a probabilistic forecast. A large system sometimes may fail to deliver reserve because of transmission congestion when there is only a system-wide reserve requirement. To account for these issues, zonal reserve requirements are presented in a simulation of the Midcontinent Independent System Operator (MISO) market considering reserve deployment with transmission constraints [25].

In contrast, scenario-based SUC determines the UC decisions to provide implicit reserves by considering a set of forecast scenarios. Papavasiliou et al. [10] compare two-stage SUC and DUC with different reserve policies. The results show that SUC can produce a lower-cost solution than DUC. This conclusion is similar to the one drawn in [8]. In [15], Uckun et al. propose an improved stochastic UC formulation which approximates a multi-stage formulation. The results show a significantly lower operational cost than traditional two-stage SUC, with a limited increase in computational burden. SUC requires a good-quality scenario set that fully characterizes the wind uncertainty. However, SUC is generally not computationally tractable, with more than 100 scenarios for a system of realistic size. Hence, scenario reduction is applied to select representative scenarios [12][26][27]. Fast forward selection performs well with regard to both economical and computational aspects [12]. Decomposition frameworks are also helpful

to address the computational challenges. We consider Benders decomposition (BD) [11] and linear-shift-factor (LSF) decomposition [28], two common approaches to improving the computational performance of UC, as discussed in Chapter 3.

IUC does not require full information about the wind power distributions, as it only uses the upper bound (UB) and lower bound (LB) for the wind power forecast. Ramping capabilities between these bounds are considered to ensure the operational feasibility in extreme situations [16]. Pandzic et al. [17] modify the IUC approach by determining the ramping requirements with a data-driven method to reduce the over-conservativeness within the original formulation. Liu et al. [18] further improve the IUC formulation with a fuzzy set approach to transform the crisp interval bounds into a fuzzy one, and show that if the wind curtailment cost is zero, then only the LB is necessary. Similarly, RUC only requires a polyhedral uncertainty set. It aims to minimize the worst-case operating cost and ensure the feasibility of all possible realizations within the set [19]-[20]. Hence, the RUC approach is by definition a very conservative operational strategy. We review different approaches to power system operations under uncertainty with renewable energy in more detail in [24].

The contribution of the present report is to systematically evaluate the impact of UC formulations, operating-reserve policies, and wind uncertainty representations on short-term power system operations in terms of economics, reliability, and computational performance. We focus the comparison on DUC, IUC, and SUC formulations with different decomposition techniques. A zonal implementation is also listed as additional constraints to improve system reliability.

The report is organized as follows: Chapter 2 describes the probabilistic forecasting techniques and scenario generation and reduction methods used in the analysis. Chapter 3 introduces details of the different UC formulations and decomposition techniques that are compared in the case study. The market simulation platform is presented in Chapter 4, and Chapter 5 presents the case study based on a modified IEEE-118 bus system. Conclusions are summarized and discussed in Chapter 6.

2 WIND POWER PROBABILISTIC FORECASTING AND REPRESENTATION

In this chapter, we present a brief introduction to probabilistic wind power forecasting as well as scenario generation and reduction methods that are typically used to generate inputs for UC models under forecast uncertainty. References with more details are provided for interested readers.

2.1 PROBABILISTIC FORECASTING

As wind uncertainty information is becoming increasingly important with higher wind penetration levels, probabilistic forecasting has drawn a lot of attention from both industry and academia in recent years [2]. Probabilistic wind forecasting methods can be categorized into two groups: parametric approaches and non-parametric approaches.

Parametric approaches assume that the wind power/speed follows a predictive density fully characterized by a parameter set. Common assumptions include Gaussian or Beta distribution [29]. Pinson [4] also proposes a modified Generalized Logit-Normal distribution to improve the uncertainty modeling.

For non-parametric approaches, there is no assumption of the distribution shape, and a set of quantiles or probability density forecasts are used to characterize the wind uncertainty information [2]. Quantile regression (QR) [5]-[6] and kernel density estimation (KDE) [3],[7] are two popular non-parametric methods. QR forecasts each desired quantile level in the probability distribution, commonly as 5%, 10%, 90% and 95%. Spline-based QR [5] and forest-based QR [6] have been demonstrated to have prediction ability without prior knowledge of the wind distribution shape. Serving as another powerful tool, KDE generates a smooth probability density function for the wind power with a sum of kernels. In order to perform well, this data-driven approach relies on tunings and cross-validation steps to select proper kernel functions, explanatory variables, and bandwidths [3],[8].

In this report, we generate probabilistic wind forecasts with a well-tuned conditional KDE method as presented in [3],[8]. We adopt a time-adaptive quantile-copula to produce the probabilistic wind power forecasts. Following the approach in [3], the point forecast and the hour of the day are used as explanatory variables in the model, which is trained on historical wind power data. Then, conditional KDE is applied to estimate the conditional wind power probability distribution. Next, the time-adaptive quantile-copula approach estimates the forecast probability density function for each time interval. We refer readers to [3] for more details.

2.2 SCENARIO GENERATION WITH SPATIO-TEMPORAL CORRELATION

From the probabilistic forecasts, we generate the wind uncertainty sets on the basis of desired confidence levels for the DUC and IUC formulations. For instance, for a 90% confidence range, we use the 5% and 95% quantiles as the LB and UB for wind power. To generate

scenarios for multiple wind farms for the SUC formulation, a spatio-temporal covariance matrix is constructed following [30]-[31].

The historic values are first transformed into a standard normal distribution domain with a nataf transformation [30]. Then, historic time series including multiple time periods and wind farm locations are obtained to build the covariance matrix. In our case, the covariance matrix has 72 dimensions, as 24 hours and 3 wind farm locations are considered for the spatio-temporal correlation. This covariance matrix is adaptively trained as time evolves.

Then, we sample a multivariate normal distribution with a zero-mean and trained covariance matrix. Each sampling produces a vector with 72 dimensions, which can be transformed back into the wind power value domain with the inverse nataf transformation. This vector represents one scenario of three wind farms' wind profile in 24 hours. We keep sampling with the same covariance matrix until the desired number of scenarios is reached. Next, we update the covariance matrix and move the scenario generation on to the next day. Readers can consult [31] for more a detailed description of procedures.

2.2 SCENARIO REDUCTION

After a large set of scenarios is sampled from the estimated probability distribution and covariance matrix, scenario reduction [26] is applied to obtain a reduced scenario set with GAMS/SCENRED [32]. As the computational burden to run stochastic optimization with more than 100 scenarios is usually intractable, the scenario reduction step is necessary to approximate the true optimal solution at the expense of slightly lower accuracy.

As discussed in [12], fast forward selection, simultaneous backward reduction, k-means clustering and importance sampling are four popular scenario reduction techniques. Fast forward selection can achieve better results, both economically and computationally, when the selected scenario number is not large. In addition, although selecting more scenarios brings more accurate approximation results, this marginal economic benefit does not make up for exponentially increased computing time. Wu et al. [13] present similar results when comparing stochastic UC with different numbers of selected scenarios.

GAMS/SCENRED provides a utility to automatically select scenarios efficiently with a combination of fast forward and backward reductions. Interested readers can refer to [32] for more material. Figure 1 shows a reduced scenario set for one sample day.

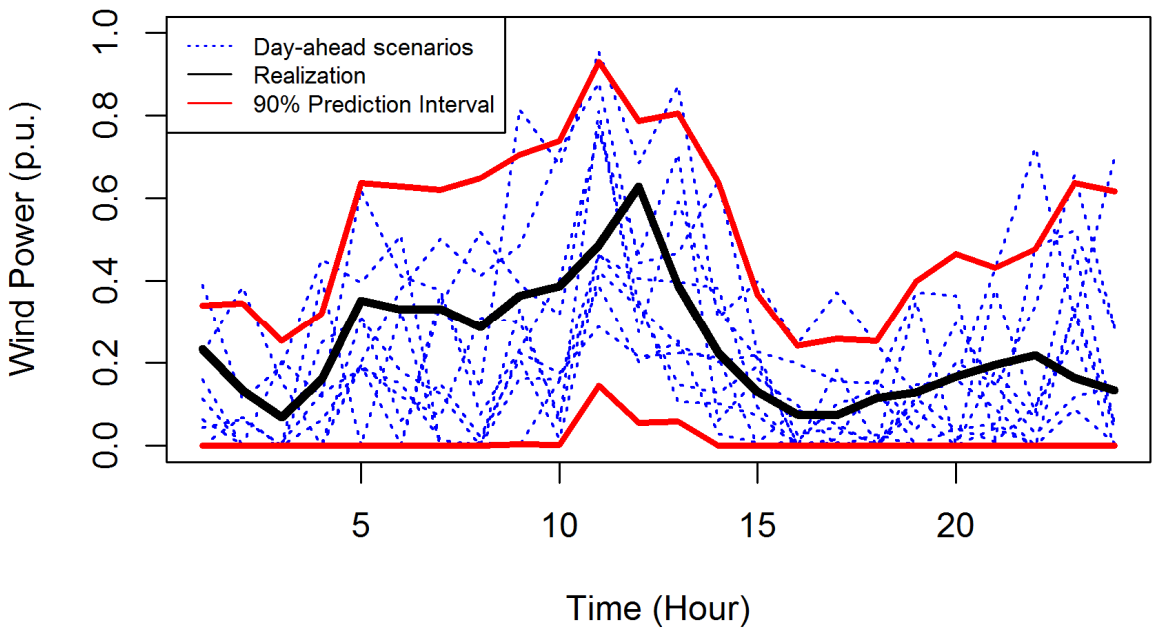

FIGURE 1 Reduced Scenarios and Confidence Interval for Wind Power.

3 METHODS AND FORMULATIONS

In this chapter, we present detailed UC formulations with different uncertainty management strategies. We first introduce the deterministic formulations with dynamic reserve strategies (DUC); then the zonal modifications (DUC-Z) are applied to further improve the reliability. Next, the extensive stochastic programming formulation (SUC-E) is provided. To improve the computational efficiency, a linear-shift-factor-based decomposition (SUC-LSF) and Benders decomposition (SUC-BD) are also discussed here. In addition, we provide the formulation with interval optimization (IUC) to determine the optimal reserve level on the basis of the given wind confidence intervals.

3.1 NOMENCLATURE

Indices and Sets:

i	Index of thermal generators
k	Index of generator cost blocks
t	Index of scheduling time periods
s	Index of scenarios
zn	Index of zones
l	Index of transmission lines
b	Index of buses
w	Index of wind farms
v	Index of decomposition iterations

Binary Decision Variables:

$u_{i,t}$	Commitment variable for generator i at time t
$y_{i,t}$	Shutdown indicator for generator i at time t
$z_{i,t}$	Start-up indicator for generator i at time t

Continuous Non-negative Decision Variables:

$csu_{i,t}$	Start-up cost for generator i at time t
$csd_{i,t}$	Shutdown cost for generator i at time t
$cpg_{i,t,s}$	Energy production cost for generator i at time t, scenario s
$creg_{i,t,s}$	Regulation reserve cost for generator i at time t, scenario s
$csr_{i,t,s}$	Spinning reserve cost for generator i at time t, scenario s
$cnsr_{i,t,s}$	Non-spinning reserve cost for generator i at time t, scenario s
$tcens_{t,s}$	Total penalty cost for unserved energy at time t, scenario s
$tcregns_{t,s}$	Total penalty cost for unserved regulation reserve at time t, scenario s
$tcrns_{t,s}$	Total penalty cost for unserved spinning reserve at time t, scenario s
$tcnrns_{t,s}$	Total penalty cost for unserved non-spinning reserve at time t, scenario s
$tcregzns_{t,zn,s}$	Total penalty cost for unserved regulation reserve at time t, zone zn, scenario s
$tcrzns_{t,zn,s}$	Total penalty cost for unserved spinning reserve at time t, zone zn, scenario s
$tcnrzns_{t,zn,s}$	Total penalty cost for unserved non-spinning reserve at time t, zone zn, scenario s
$p_{i,t,s}$	Dispatched power output for generator i at time t, scenario s
$delta_{i,k,t,s}$	Dispatched power output at block k for generator i at time t, scenario s
$wg_{w,t,s}$	Scheduled wind output for wind farm w at time t, scenario s
$regup_{i,t,s}$	Regulation up reserve for generator i at time t, scenario s
$regdn_{i,t,s}$	Regulation down reserve for generator i at time t, scenario s
$sr_{i,t,s}$	Spinning reserve for generator i at time t, scenario s
$nsrn_{i,t,s}$	Non-spinning reserve when the unit is on for generator i at time t, scenario s
$nsrf_{i,t,s}$	Non-spinning reserve when the unit is off for generator i at time t, scenario s
$ens_{b,t,s}$	Amount of non-served energy at bus b, time t, scenario s
$runs_{t,s}$	Amount of non-served up regulation reserve at time t, scenario s
$rdns_{t,s}$	Amount of non-served down regulation reserve at time t, scenario s
$rns_{t,s}$	Amount of non-served spinning reserve at time t, scenario s
$nrns_{t,s}$	Amount of non-served non-spinning reserve at time t, scenario s;
$ruzns_{t,zn,s}$	Amount of non-served up regulation reserve at time t, zone zn, scenario s
$rdzns_{t,zn,s}$	Amount of non-served down regulation reserve at time t, zone zn, scenario s
$rzns_{t,zn,s}$	Amount of non-served spinning reserve at time t, zone zn, scenario s
$nrzns_{t,zn,s}$	Amount of non-served non-spinning reserve at time t, zone zn, scenario s
α	Auxiliary variable to compute total cost during BD
α_s	Optimal dispatch cost for scenario s during BD
$slack_s$	Slack variables at scenario s
$p_{i,t}^c$	Corrective generation for IUC for generator i at time t
$wg_{w,t}^c$	Corrective wind dispatch for IUC for wind farm w at time t

Parameters:

$PROB_s$	Probability for scenario s
SUC_i	Start-up cost for generator i
SDC_i	Shutdown cost for generator i
NLC_i	No-load cost for generator i
$MC_{i,k}$	Marginal cost for generator i at cost segment k
$COSTREG_i$	Regulation reserve cost for generator i
$COSTSR_i$	Spinning reserve cost for generator i
$COSTNSR_i$	Non-spinning reserve cost for generator i
$CENS$	Cost of unserved energy
$CRGNS$	Cost of unserved regulation reserve
$CRNS$	Cost of unserved spinning reserve
$CNRNS$	Cost of unserved non-spinning reserve
$D_{b,t}$	Load at bus b at time t
LSF_b^l	Linear-Shift-Factor for line l at bus b
$U(b)$	Resources connected at bus b
$LINE_l^{cap}$	Real power capacity for line l
$REGRATIO$	Regulation reserve ratio in the total reserve amount
$SRRATIO$	Spinning reserve ratio in the total reserve amount
$RCON_t$	Contingency reserve amount at time t
$RW_{w,t,s}$	Dynamic reserve amount from wind w at time t, scenario s
MUT_i	Minimum up time for generator i
MDT_i	Minimum down time for generator i
$PMIN_i$	Minimum generation level for generator i
$PMAX_i$	Maximum generation level for generator i
$PR_{i,k}$	Power capacity for generator i at cost segment k
RSU_i	Start-up ramp limit for generator i
RSD_i	Shutdown ramp limit for generator i
RU_i	Ramp up limit for generator i
RD_i	Ramp down limit for generator i
$REGRT_i$	Regulation reserve responsive time for generator i
$SRRT_i$	Spinning reserve responsive time for generator i
$NSRRT_i$	Non-spinning reserve responsive time for generator i
MSR_i	Minute spinning reserve rate for generator i
QSC_i	Quick-start generation capability for generator i
PO_i	Initial power generation level for generator i
UO_i	Initial commitment status for generator i
$WG_{w,t,s}$	Forecast wind generation for wind farm w at time t, scenario s (denoted as central forecast in DUC case)
F_s^v	Optimality dispatch cost at BD iteration v, scenario s
$DualU_{i,t,s}^v$	Dual variable for fixing $u_{i,t}$ at BD iteration v, scenario s
$DualY_{i,t,s}^v$	Dual variable for fixing $y_{i,t}$ at BD iteration v, scenario s
$DualZ_{i,t,s}^v$	Dual variable for fixing $z_{i,t}$ at BD iteration v, scenario s
$TempU_{i,t}^v$	Temporary solution of $u_{i,t}$ at BD iteration v
$TempY_{i,t}^v$	Temporary solution of $y_{i,t}$ at BD iteration v
$TempZ_{i,t}^v$	Temporary solution of $z_{i,t}$ at BD iteration v
$WG_{w,t}^{LB}$	Forecast wind generation LB for wind farm w at time t

3.2 DETERMINISTIC FORMULATION WITH DYNAMIC RESERVE STRATEGIES

DUC is the current industry practice and there are many papers devoted to improving the computational issues for DUC formulations, e.g., [33]-[35]. Compared to other formulations as presented in [33]-[34], Morales-Espana's formulation [35] is tight and compact and can be efficiently solved with current commercial MILP solvers. Therefore, we adopt this formulation [35] as the core UC formulation, and extra constraints are added to achieve additional functions. We model multiple reserve products including the regulation up/down, spinning, non-spinning reserve and corresponding zonal reserve products.

A. Objective Function

min

$$\sum_{i,t}(csu_{i,t} + csd_{i,t}) \tag{3.1}$$

$$+\sum_{s} PROB_s(\sum_{i,t}(cpg_{i,t,s} + creg_{i,t,s} + csr_{i,t,s} + cnsr_{i,t,s})$$

$$+\sum_{t}(tcens_{t,s} + tcregns_{t,s} + tcrns_{t,s} + tcnrns_{t,s})$$

$$+\sum_{zn,t}(tcregzns_{t,zn,s} + tcrzns_{t,zn,s} + tcnrzns_{t,zn,s}))$$

Cost components:

$$csu_{i,t} \geq SUC_i \cdot z_{i,t} \tag{3.2}$$

$$csd_{i,t} \geq SDC_i \cdot y_{i,t} \tag{3.3}$$

$$cpg_{i,t,s} = NLC_i \cdot u_{i,t} + \sum_{k} MC_{i,k} \cdot delta_{i,k,t,s} \tag{3.4}$$

$$creg_{i,t,s} = COSTREG_i \cdot (regup_{i,t,s} + regdn_{i,t,s}) \tag{3.5}$$

$$csr_{i,t,s} = COSTSR_i \cdot sr_{i,t,s} \tag{3.6}$$

$$cnsr_{i,t,s} = COSTSR_i \cdot (nsrn_{i,t,s} + nsrf_{i,t,s}) \tag{3.7}$$

$$tcens_{t,s} = CENS \cdot \sum_{b} ens_{b,t,s} \tag{3.8}$$

$$tcregns_{t,s} = CRGNS \cdot (runs_{t,s} + rdns_{t,s}) \tag{3.9}$$

$$tcrns_{t,s} = CRNS \cdot rns_{t,s} \tag{3.10}$$

$$tcnrns_{t,s} = CNRNS \cdot nrns_{t,s} \tag{3.11}$$

$$tcregzns_{zn,t,s} = CRGNS \cdot (ruzns_{t,zn,s} + rdzns_{t,zn,s}) \tag{3.12}$$

$$tcrzns_{zn,t,s} = CRNS \cdot rzns_{t,zn,s} \tag{3.13}$$

$$tcnrzns_{zn,t,s} = CNRNS \cdot nrzns_{t,zn,s} \tag{3.14}$$

As shown in equation (3.1), the DUC model minimizes the sum of start-up and shutdown costs (first row), fuel costs and reserve costs (second row), and penalties for the violations (third row). If zonal reserve is implemented, the corresponding penalty terms (fourth row) are added in the objective function. In the DUC settings, there is only one scenario, and its probability is 1. We include the scenario index, *s*, in the equations above since we use the same equations to describe the SUC models in sections 3.2 and 3.3. Equations (3.2)–(3.14) describe the calculation for each cost component. Note that there is no penalty cost for wind curtailment.

B. Power System Operational Requirements

Power balance constraint:

$$\sum_i p_{i,t,s} + \sum_w wg_{w,t,s} = \sum_b (D_{b,t} - ens_{b,t,s}) \tag{3.15}$$

Power flow constraint:

$$pf_{l,t,s} = \sum_b LSF_b^l \cdot (\sum_{i \in U(b)} p_{i,t,s} + \sum_{w \in U(b)} wg_{w,t,s} - (D_{b,t} - ens_{b,t,s})) \tag{3.16}$$

$$-LINE_l^{cap} \leq pf_{l,t,s} \leq LINE_l^{cap} \tag{3.17}$$

Market regulation up/down reserve requirement:

$$runs_{t,s} + \sum_i regup_{i,t,s} \geq REGRATIO \cdot (RCON_t + \sum_w RW_{w,t,s}) \tag{3.18}$$

$$rdns_{t,s} + \sum_i regdn_{i,t,s} \geq REGRATIO \cdot (RCON_t + \sum_w RW_{w,t,s}) \tag{3.19}$$

Market spinning reserve requirement:

$$rns_{t,s} + \sum_{i} regup_{i,t,s} + \sum_{i} sr_{i,t,s} \geq (REGRATIO + SRRATIO) \cdot (RCON_t + \sum_{w} RW_{w,t,s}) \tag{3.20}$$

Market non-spinning reserve requirement

$$nrns_{t,s} + \sum_{i} regup_{i,t,s} + \sum_{i} sr_{i,t,s} + \sum_{i} nsrn_{i,t,s} + \sum_{i} nsrf_{i,t,s} \geq (RCON_t + \sum_{w} RW_{w,t,s}) \tag{3.21}$$

Zonal regulation up/down reserve requirement:

$$ruzns_{t,zn,s} + \sum_{i \in zn} regup_{i,t,s} \geq REGRATIO \cdot \sum_{w \in zn} RW_{w,t,s} \tag{3.22}$$

$$rdzns_{t,zn,s} + \sum_{i \in zn} regdn_{i,t,s} \geq REGRATIO \cdot \sum_{w \in zn} RW_{w,t,s}$$

Zonal spinning reserve requirement:

$$rzns_{t,zn,s} + \sum_{i \in zn} regup_{i,t,s} + \sum_{i \in zn} sr_{i,t,s} \geq (REGRATIO + SRRATIO) \cdot \sum_{w \in zn} RW_{w,t,s} \tag{3.23}$$

Zonal non-spinning reserve requirement

$$nrzns_{t,zn,s} + \sum_{i \in zn} regup_{i,t,s} + \sum_{i \in zn} sr_{i,t,s} + \sum_{i \in zn} nsrn_{i,t,s} + \sum_{i \in zn} nsrf_{i,t,s} \geq \sum_{w \in zn} RW_{w,t,s} \tag{3.24}$$

Equations (3.15-3.24) represent the constraints related to the system operation constraints as described in [8][28][35]. The market and zonal reserve implementation follows the one described for MISO [25]. The higher-quality reserve product is able to substitute for low-quality products. As regulation reserve has the strictest time requirement (i.e., how quickly the reserve capacity has to respond), it is the highest-quality reserve product, followed by spinning reserve and non-spinning reserve. The dynamic reserve amount is determined from the probabilistic wind power forecast; normally, we choose the 10%, 5% or 1% quantile to hedge against over-forecasting. The sum of this dynamic reserve and a fixed contingency reserve satisfies the

system-wide total operating-reserve requirements. Regulation up/down, spinning and non-spinning reserve requirements are determined as fixed fractions of the total reserve requirements. The percentages are obtained from PJM historical data statistics [36].

C. Thermal Unit Constraints

Generator logical constraint:

$$u_{i,t} - u_{i,t-1} = z_{i,t} - y_{i,t} \tag{3.25}$$

Minimum up and down time:

$$\sum_{tt=t-MUT_i+1}^{t} z_{i,tt} \leq u_{i,t} \tag{3.26}$$

$$\sum_{tt=t-MDT_i+1}^{t} y_{i,tt} \leq 1 - u_{i,t} \tag{3.27}$$

Generation block constraints:

$$p_{i,t,s} = PMIN_i \cdot u_{i,t} + \sum_k delta_{i,k,t,s} \tag{3.28}$$

$$delta_{i,k,t,s} \leq PR_{i,k} \tag{3.29}$$

Generation limits with minimum for t = 1:

$$\sum_k delta_{i,k,t,s} + regup_{i,t,s} + sr_{i,t,s} + nsrn_{i,t,s} \leq (PMAX_i - PMIN_i) \cdot u_{i,t} - (PMAX_i - RSU_i) \cdot z_{i,t} \tag{3.30}$$

$$\sum_k delta_{i,k,t,s} + regup_{i,t,s} + sr_{i,t,s} + nsrn_{i,t,s} \leq (PMAX_i - PMIN_i) \cdot u_{i,t} - (PMAX_i - RSD_i) \cdot y_{i,t+1} \tag{3.31}$$

Generation limits with minimum for t > 1:

$$\sum_k delta_{i,k,t,s} + regup_{i,t,s} + sr_{i,t,s} + nsrn_{i,t,s} \leq (PMAX_i - PMIN_i) \cdot u_{i,t} - (PMAX_i - RSU_i) \cdot z_{i,t} - (PMAX_i - RSD_i) \cdot y_{i,t+1} \tag{3.32}$$

Regulation reserve rate:

$$regup_{i,t,s} \leq REGRT_i \cdot MSR_i \cdot u_{i,t} \tag{3.33}$$

$$regdn_{i,t,s} \leq REGRT_i \cdot MSR_i \cdot u_{i,t} \tag{3.34}$$

Spinning reserve rate:

$$sr_{i,t,s} \leq SRRT_i \cdot MSR_i \cdot u_{i,t} \tag{3.35}$$

Non-spinning reserve rate:

$$nsrn_{i,t,s} \leq NSRRT_i \cdot MSR_i \cdot u_{i,t} \tag{3.36}$$

$$nsrf_{i,t,s} \leq QSC_i \cdot (1 - u_{i,t}) \tag{3.37}$$

Ramp rate for t > 1:

$$(p_{i,t,s} - p_{i,t-1,s}) + regup_{i,t,s} + sr_{i,t,s} + nsrn_{i,t,s} \leq RU_i \tag{3.38}$$

$$(p_{i,t-1,s} - p_{i,t,s}) + regdn_{i,t,s} \leq RD_i \tag{3.39}$$

Ramp rate for t = 1:

$$(p_{i,t,s} - PO_i) + regup_{i,t,s} + sr_{i,t,s} + nsrn_{i,t,s} \leq RU_i \cdot UO_i + RSU_i \cdot z_{i,t} \tag{3.40}$$

$$(PO_i - p_{i,t,s}) + regdn_{i,t,s} \leq RD_i \cdot u_{i,t} + RSD_i \cdot y_{i,t} \tag{3.41}$$

Equations (3.25) to (3.41) represent all generation constraints of the UC model, including minimum/maximum generation limits, ramping constraints, UC logic, minimum up/down time and reserve rate [35]. Ramp constraints and generation limits are specifically formulated in a tight and compact form.

D. Wind Power Constraints

$$wg_{w,t,s} \leq WG_{w,t,s} \tag{3.42}$$

Equation (3.42) represents the wind dispatch constraint, i.e. the wind can be curtailed below the forecasted level of available generation.

E. Summary

The previous sections, 3.2 A–D, presented the DUC optimization model based on [8][28][35]. The dynamic reserve is enforced at the system level to schedule the thermal generators in positions so that they can easily ramp up and down to mitigate the wind forecast errors. In addition, the zonal reserve settings can be added to improve the reserve deliverability when wind farms are located in different zones.

3.3 STOCHASTIC PROGRAMMING-BASED FORMULATION

The extensive stochastic programming-based formulation is similar to the deterministic formulation we presented above in section 3.2. The major difference is that the DUC model only includes one scenario, whereas the SUC formulation includes multiple wind power scenarios and minimizes the expected cost across the scenarios. Different scenarios are assigned with different probabilities. Hence, the produced schedule can hedge against wind variations within the properly constructed scenario set.

One of the most important features of SUC is the implicit scheduling of reserves rather than imposing explicit reserve requirements. Large operating reserve reqirements are therefore not necessary and are uneconomical under SUC. In fact, most SUC formulations [11][12] remove reserve products completely. However, as shown in [8], adding a small amount of dynamic reserve may actually boost the system's economic performance without adding computing time. The reason is that the additional dynamic reserve hedges agains uncertainty not captured in the reduced scenario set used as input to the SUC model. In our formulation, we follow the approach used in [8] and add additional dynamic reserves equal to a small portion of wind power per scenario. Since contingency reserves are deployed for contingencies only, and to correct wind power forecasting errors, we do not modify this reserve amount. The full reserve formulations, including the zonal parts, still follow equations (3.18)–(3.24). Note that the dynamic reserve amount, $RW_{w,t,s}$, has been reduced and it can also be set to zero, as done in many traditional SUC studies.

3.4 STOCHASTIC PROGRAMMING FORMULATION WITH DECOMPOSITION METHODS

The solution quality of scenario-based SUC formulations depends on the quality of the scenario set. A larger scenario set produces a more accurate schedule at the expense of a higher computational burden. To overcome the computational obstacle, many decomposition algorithms have been proposed, including LSF decomposition [28], BD [16][28], progressive hedging [14], dual decomposition [37] and many more. In this report, we only focus on the LSF decomposition and BD, as they are relatively straightforward and no tuning is necessary, unlike the progressive hedging approach.

3.4.1 Linear-Shift-Factor Decomposition

When the system is large, it is computationally expensive to evaluate the power flow limits for all lines. As shown in [28], the number of congested lines during operations is typically only a small fraction of the full line set. Therefore, considering only critical line flow limits can improve computational performances without sacrificing solution accuracy. This assumption also reflects real-world ISO practice: In [38], only a selected number of lines are labeled with "Monitor Flag" to check their line limit during operation, and other line limits are not evaluated in the constraints.

In the SUC problem, considering the number of lines, hours and scenarios, only a few transmission constraints are actually binding. Therefore, applying LSF decomposition can effectively relieve the computational burden, as checking flow limits is essentially a linear programming (LP) feasibility problem, which can be solved very efficiently. This SUC requires minimum effort to change from the original extensive form. The pseudo code is as follows:

Algorithm 1: LSF Decomposition:

1) Initialize the line checking set O (l, t, s) as an empty set;
2) Solve the SUC problem with network constraints (3.17) only imposed on the line checking set O;
3) Evaluate all the remaining line tuples (l, t, s) for their flow limits: if no limits are violated, go to step 4); else, add the violated line tuples (l, t, s) in O, and go to step 2);
4) Stop the program, and output the result.

3.4.2 Benders Decomposition

For the two-stage SUC structure, as the second-stage economic dispatch problem per scenario is an LP problem, the BD method can be applied here. The SUC problem is suitable to decompose into a master problem and a collection of subproblems for each scenario. The master problem involves all the UC constraints and Benders cuts. In the classical Benders approach, the subproblems, with the dispatch constraints [13], are used to generate feasibility and optimality cuts for the master problem to converge. However, the convergence rate can be slow. Similarly to the approach in [11], we only consider the optimality subproblems, and slack variables are added to form complete second-stage recourse decisions. In each iteration, the subproblems evaluate the dispatch decision on the basis of commitment status sent from the master problem, and return sensitivities to generate Benders cuts for the master solution. In the master problem, we add an online generation capacity constraint and an aggregate optimality cut summing all optimality cuts together to further improve the convergence. The pseudo code is provided below, with more detailed descriptions of the acceleration techniques provided in [28].

Algorithm 2 - Benders Decomposition:

1) Initialize the problem, UB=+∞, LB= –∞;
2) Solve master problem, update the LB with objective function LB=z_{LB};
3) Run optimality subproblem for each scenario: update the UB with solution from optimality subproblems UB = z_{UB};
4) Check the convergence: if |UB – LB|≤ ε , go to step 5); else, generate optimality cuts and return to step 2);
5) Stop the program, and output the results.

A. Master problem

Objective function:

min

$$z_{LB} = \sum_{i,t} (csu_{i,t} + csd_{i,t}) + \alpha \tag{3.43}$$

Start-up and shutdown cost:

(3.2), (3.3)

Generator logical constraint:

(3.25)

Minimum up and down time:

(3.26), (3.27)

Optimality cuts:

$$\begin{aligned} \alpha_s \geq F_s^{v-1} &+ \sum_{i,t} DualU_{i,t,s}^{v-1} \cdot (u_{i,t} - TempU_{i,t}^{v-1}) \\ &+ \sum_{i,t} DualY_{i,t,s}^{v-1} \cdot (y_{i,t} - TempY_{i,t}^{v-1}) \\ &+ \sum_{i,t} DualZ_{i,t,s}^{v-1} \cdot (z_{i,t} - TempZ_{i,t}^{v-1}) \end{aligned} \tag{3.44}$$

Aggregate optimality cuts:

$$\alpha \geq \sum_{s} PROB_s \cdot F_s^{v-1} + \sum_{i,t,s} PROB_s \cdot DualU_{i,t,s}^{v-1} \cdot (u_{i,t} - TempU_{i,t}^{v-1}) + \sum_{i,t,s} PROB_s \cdot DualY_{i,t,s}^{v-1} \cdot (y_{i,t} - TempY_{i,t}^{v-1}) + \sum_{i,t,s} PROB_s \cdot DualZ_{i,t,s}^{v-1} \cdot (z_{i,t} - TempZ_{i,t}^{v-1}) \tag{3.45}$$

System generation availability constraint:

$$\sum_{i} PMAX_i \cdot u_{i,t} + \sum_{w} W_{w,t,s} \geq \sum_{b} D_{b,t} + \sum_{w} RW_{w,t,s} + RCON_t \tag{3.46}$$

In addition to the generator UC constraint (3.25)–(3.27), constraints (3.44)–(3.46) are added to calculate the objective function component for the master problem with optimality cuts. Equation (3.45) is the classic Benders optimality cuts with dual information from the scenario optimality subproblem. Note that $DualU_{i,t,s}^{v}$, $DualY_{i,t,s}^{v}$ and $DualZ_{i,t,s}^{v}$ are the duals of constraints (3.48)–(3.50) from subproblem s at iteration v.

Rather than iterating with feasibility cuts, (3.46) is used to quickly throw away solutions far away from optimal solutions. This constraint ensures that sufficient system generation capacity is available at any time. For a feasible solution, this valid inequality always holds, which helps the solver cut infeasible solutions efficiently. A slack variable with penalty cost could also be added in the formulation to consider situations where a very small amount of load shedding is optimal from a cost perspective.

Wen et al. [39] show that aggregate feasibility cuts accelerate BD convergence for analyzing energy storage capability to ensure system security. We adopt a similar idea to add an aggregate optimality cut in the master problem after each iteration. It indeed improves the computational performance.

B. Scenario Optimality Subproblem

Objective function:

min

$$F_s^v = \sum_{i,t} (cpg_{i,t,s} + creg_{i,t,s} + csr_{i,t,s} + cnsr_{i,t,s}) \tag{3.47}$$

$$+\sum_{t}(tcens_{t,s}+tcregns_{t,s}+tcrns_{t,s}+tcnrns_{t,s})$$

$$+\sum_{zn,t}(tcregzns_{t,zn,s}+tcrzns_{t,zn,s}+tcnrzns_{t,zn,s})$$

$$+CENS\cdot slack_s$$

Dispatch and penalty costs:

(3.4)–(3.14)

Dispatch constraints:

(3.15)–(3.24), (3.28)–(3.42)

Fix first-stage binary variables:

$$u_{i,t}=TempU_{i,t}^{v} \tag{3.48}$$

$$y_{i,t}=TempY_{i,t}^{v} \tag{3.49}$$

$$z_{i,t}=TempZ_{i,t}^{v} \tag{3.50}$$

Update the BD UB after all scenario subproblems have finished:

$$z_{UB}=\sum_{i,t}(csu_{i,t}+csd_{i,t})+\sum_{s}PROB_s\cdot F_s^{v} \tag{3.51}$$

In addition to the original dispatch and penalty cost components, additional penalty costs for the slack variables are added in the optimality subproblem objective function. After adding this term, each second-stage problem is an LP problem with complete recourse (i.e., always feasible). In the formulation above, we compactly state this slack variable as $slack_s$ in the objective function (3.47), with a penalty equation to represent the cost of energy not served, *CENS*. Such slack variables can be added to any inequality constraints. During our simulations, we found that it was only necessary to introduce additional slack variables for the generator ramp rate constraints. Note that the original formulation already has slack variables for unserved energy and reserves, with corresponding penalties included in the objective function (3.1).

Equations (3.48)–(3.50) are included in the subproblem to pass the information from the first stage. Here, we adopt a primal way to optimize the subproblems, as it is effortless for implementation. It should be noted that this optimization can also be represented with its dual problem, but it is outside the scope of this report. Interested readers can refer to [40] for more details on this topic.

3.5 INTERVAL OPTIMIZATION-BASED FORMULATION

Even with decomposition techniques, the SUC computation time is still very high compared to DUC. As presented in [16]–[[18], the IUC formulation is computationally efficient and hedges wind uncertainty well, within a certain range of uncertainty. In this report, we adopt the formulation of Liu et al. [18]. In this formulation, only the lower interval bound for wind power and corresponding transitions is considered, as it represents the worst-case situation, as proven in the appendix in [18].

Compared to DUC, the objective is still to minimize the operational cost in the normal state. Only a set of corrective action constraints is added in the formulation to ensure feasibility within the forecast interval. In the case study chapter, we find that these additional constraints do not increase the computing time compared to DUC. Similarly to SUC, the contingency reserve is kept and the reserve for wind generation uncertainty is scheduled implicitly.

Objective Function:

$$\min \quad \sum_{i,t}(csu_{i,t} + csd_{i,t}) + \sum_{i,t}(cpg_{i,t,s} + creg_{i,t,s} + csr_{i,t,s} + cnsr_{i,t,s}) \tag{3.52}$$

$$+ \sum_{t}(tcens_{t,s} + tcregns_{t,s} + tcrns_{t,s} + tcnrns_{t,s})$$

Cost components:

(3.2)–(3.11)

UC and power flow constraints at normal state:

(3.15)–(3.21), (3.25)–(3.42)

Wind corrective case:

$$wg^{c}_{w,t} \leq WG^{LB}_{w,t} \tag{3.53}$$

Power balance corrective case:

$$\sum_{i} p^{c}_{i,t} + \sum_{w} wg^{c}_{w,t} = \sum_{b} D_{b,t} \tag{3.54}$$

Generation corrective distance:

$$-regdn_{i,t,s} \leq p^{c}_{i,t} - p_{i,t,s} \leq sr_{i,t,s} + regup_{i,t,s} \tag{3.55}$$

$$-RD_i \leq p^{c}_{i,t} - p^{c}_{i,t-1} \leq RU_i \tag{3.56}$$

Transmission constraints corrective case:

$$-LINE_l^{cap} \leq \sum_b LSF_b^l \cdot (\sum_{i \in U(b)} p_{i,t}^c + \sum_{w \in U(b)} wg_{w,t}^c - D_{b,t}) \leq LINE_l^{cap} \tag{3.57}$$

Noted that although the scenario subscript, *s*, is used here, only one scenario is modeled in the IUC formulation. Equations (3.53)–(3.57) ensure the system security when the worst-case wind occurs, i.e., wind producing at the LB of the forecast interval. In addition, (3.56) ensures that the system has enough reserve to move to the new feasible dispatch state during this worst case. These additional constraints force the system to buy additional reserves to guarantee the worst-case feasibility.

4 TEST SYSTEM AND DATA

In this chapter, we will introduce the test system and data used for the case study. The simulation settings are also described, to facilitate reproducibility of the work.

4.1 IEEE 118-BUS SYSTEM

The modified IEEE 118-bus system [41] is applied as the test system for the work. There are a total of 118 buses, 54 generators, 186 transmission lines and 91 load demands. The one-line diagram is shown in Figure 2 [42]:

4.2 LOAD DEMAND AND GENERATION SUPPLY

In the IEEE 118-bus test system, there are a total of 54 thermal generators, including 21 quick-start units. The total generation capacity is 7220 MW, of which 650 MW is from quick-start units. The whole generation portfolio includes 21 gas/oil units and 33 coal units. The generator cost data originate from the 118-bus system with piecewise cost curves. The reserve costs are computed on the basis of historical data from the PJM reserves market. Rather than having each generator provide its own unique reserve bid, we set a system-wide offer price for

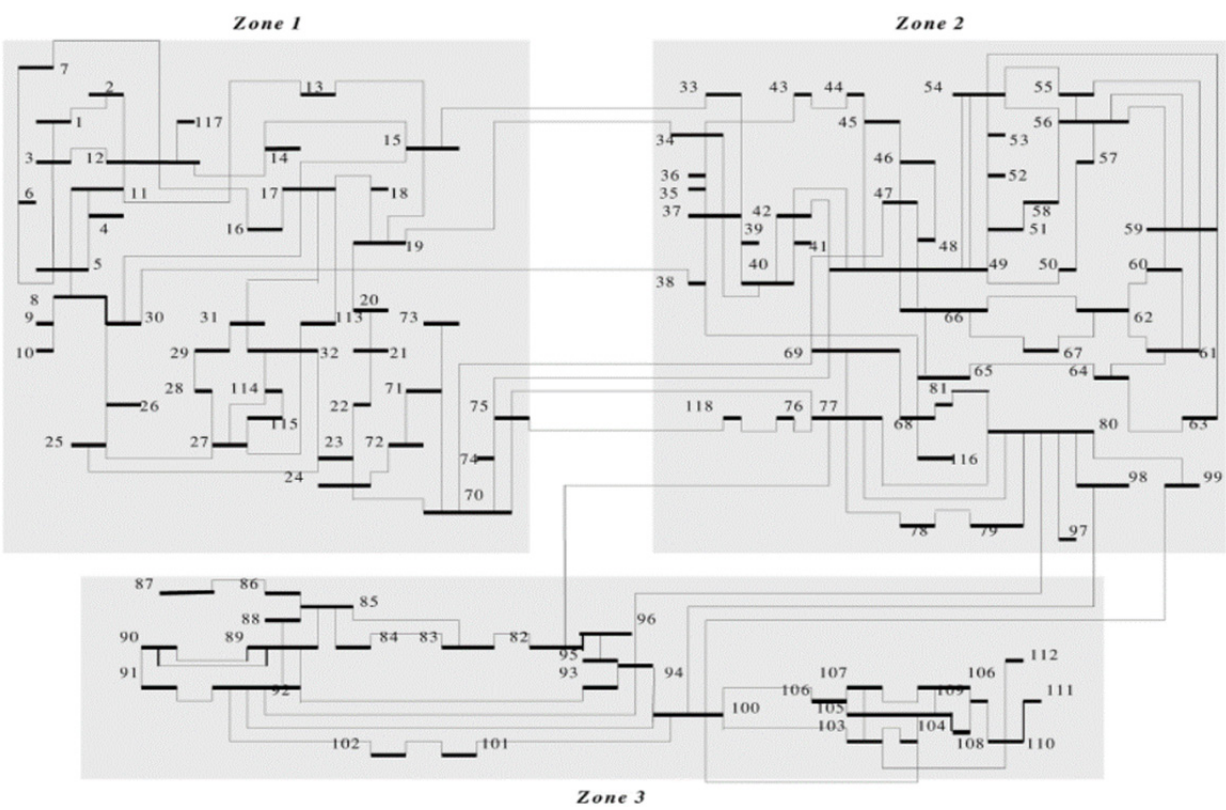

FIGURE 2 IEEE-118 System One-line Diagram

all generators. The assumed bid costs for regulation services, spinning reserve, and non-spinning reserve are 10 $/MW, 2.88 $/MW and 0.70 $/MW, respectively [36].

There are a total of 91 load buses, with hourly loads following a fixed ratio based on the total system demand. The original 118-bus system load is scaled on the basis of actual load profiles from the U.S. state of Illinois in 2006. The system peak load is 6616 MW and the average load is 4093 MW in the four-month simulation period from July to October. The summer season from July to August represents a heavy-load season with peak load of 6616 MW and average load of 4535 MW. In contrast, the fall season from September to October represents a light-load season with peak load of 4722 MW and average load of 3645 MW.

4.3 TRANSMISSION NETWORK

There are 186 lines in the system, and the total transmission capacity is 45,265 MW. Within all lines, the maximum value of the line rating is 500 MW, the minimum value of the line rating is 175 MW, and the average value of the line rating is 243 MW. The DC approximation is applied to compute the active power flow with the LSF approach, as explained in the previous chapter.

4.4 ZONAL SETTING

There are three zones in the system, as shown in Figure 2. The bus numbers and load ratios are shown in Table 1.

4.5 WIND FARM DEPLOYMENT

We assume that there are three wind farms located at buses 15, 54, and 96, i.e., one in each zone. The installed wind capacity is 902.6, 911.4, and 1232.2 MW, respectively. With this wind capacity, the average available wind energy is 21% of the average load. The wind profiles are selected from the Eastern Wind Integration Dataset [43]. In order to capture the spatial correlation, the selected wind farms are all located within the state of Illinois, with a correlation of more than 0.75 in the hourly time series of wind power availability.

TABLE 1 IEEE 118 Zonal Information

	Number of Buses	Total Load Ratio
Zone 1	42	0.308
Zone 2	48	0.493
Zone 3	28	0.199
Total	118	1

4.6 DECISION FRAMEWORK

The simulation is based on a rolling decision-making process, which is typically applied in U.S. electricity markets. This includes the Day-ahead (DA) UC (DA-UC), Reliability Assessment Commitment (RAC), and Real-time (RT) Economic Dispatch (RT-ED), with updated forecast information applied at each stage. In DA-UC, the UC schedule for the day ahead is determined and passed on to the RAC stage. In RAC, the slow generators follow the DA schedule, whereas quick-start generators are allowed to adjust their status on the basis of the updated forecast. This schedule update passes to the RT-ED for the actual dispatch solution. This final dispatch then passes to the next day's simulation as the initial condition. DA-UC and RAC consider full reserve constraints on the basis of the available wind power forecast and corresponding scenarios. In contrast, the RT-ED procures the contingency reserve only, under the assumption that the wind power uncertainty has been resolved at this stage. The flowchart for the simulation is presented in Figure 3. A four-month out-of-sample simulation is carried out for the different operational strategies to cover daily, weekly, and seasonal patterns of loads and wind resource availability.

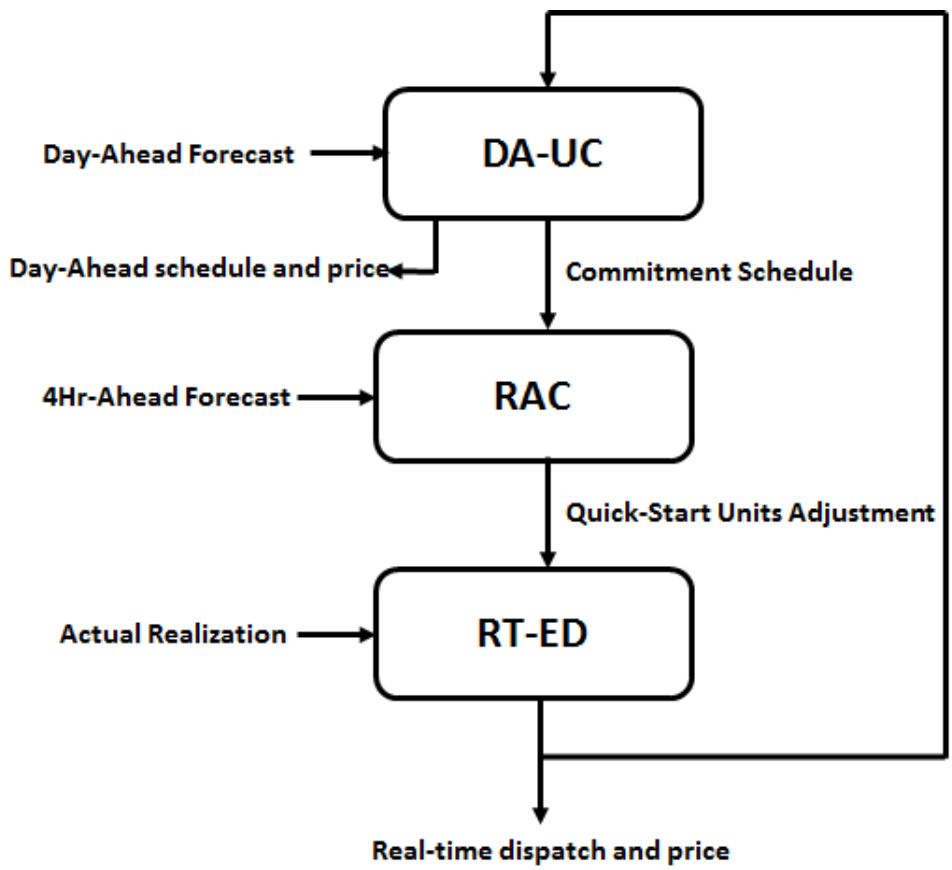

FIGURE 3 Decision-making Processes

4.7 SIMULATION SETTINGS

The DA forecast is used as the initial forecast for the DA-UC stage, and the four-hour-ahead forecast is used as the forecast for the RAC stage. Out-of-sample, actual wind realizations are applied at the RT-ED stage to evaluate the UC performance. Probabilistic forecasts for the three wind farms are first generated, then 1000 scenarios are sampled each day considering spatio-temporal correlations, with a reduced scenario set of 10 selected, as explained in chaper 2. We use 10 scenarios primarily to limit the computational burden, especially for the SUC extensive-form model. However, the extra economic benefits of more scenarios are also limited. In the case study, regulation up/down equals 15% of the total reserve requirement, while spinning and non-spinning reserve each takes 42.5% of the total requirement.

The framework is implemented in AMPL [44] and the mixed integer programming (MIP) solver is IBM ILOG CPLEX 12.1 [45] with a 0.1% optimality gap. For BD, 0.1% is the gap for the UB and LB convergence rate, and a MIP gap of 1% is used for each master problem. All the results are obtained on a Linux-based server at Argonne National Laboratory with 2x Intel E5430 Xeon CPUs and 32 GB of RAM.

5 RESULTS AND ANALYSIS

In this chapter, we present the results comparing different UC formulations. Both DA and RT results are evaluated to illustrate the various features and implications of the UC formulations. We first present production cost results. The load curtailment, reserve shedding, and wind curtailment results are also shown. Last, the computational times are compared to further demonstrate the differences between the UC models.

5.1 CASE STUDY DESCRIPTION

The DUC cases with perfect wind forecast (DUC-perfect) and point forecast (DUC-point) are selected as the two reference cases. The point forecast is obtained as the 50% quantile from the probabilistic wind power forecast. In these two reference cases, only the contingency reserve is imposed at all stages. For the DUC with dynamic reserve (DUC-DR), we choose the difference between the 50% and a lower quantile as the dynamic reserve quantity. Correspondingly, the lower quantile is also chosen as the LB for the IUC formulation. Sensitivity analysis considers multiple lower quantiles, including 40%, 30%, 20%, 10%, 5%, and 1%. The results show that using the 20% quantile is more economical than using other lower quantiles, as the benefits of the dynamic reserve cannot compensate for the additional reserve costs for lower quantiles. In the SUC cases, in addition to the different solution techniques, we compared different levels of additional wind reserve (0, 1%, 5% and 10% of wind power in each scenario).

Table 2 shows all the case descriptions that are used in the case study.

5.2 PRODUCTION COST

5.2.1 Day-ahead Costs

We first present results for DA total costs (energy production costs, load-shedding penalty, reserve cost and reserve curtailment penalty) and total energy costs (energy production costs and load-shedding penalty) for summer (July and August) and fall (September and October) in Tables 3–6. “Total costs” compares the operational cost as expressed in the objective function, whereas total energy cost represents the unit scheduling cost and load-shedding penalty only, without considering the costs of reserves. As the reserve requirements are different in the different cases, we present both cost figures for a better illustration of cost performances under different formulations. DUC-perfect always produces the cheapest solution, as expected given the perfect-forecast assumption.

TABLE 2 Case Description. All cases use a 21% available wind penetration

Case Number	Description
DUC-perfect	Deterministic UC with perfect forecast
DUC-point	Deterministic UC with deterministic forecast
DUC-DR-40	Deterministic UC with deterministic forecast, dynamic reserve with 50%–40% quantile
DUC-DR-30	Deterministic UC with deterministic forecast, dynamic reserve with 50%–30% quantile
DUC-DR-20	Deterministic UC with deterministic forecast, dynamic reserve with 50%–20% quantile
DUC-DR-10	Deterministic UC with deterministic forecast, dynamic reserve with 50%–10% quantile
DUC-DR-5	Deterministic UC with deterministic forecast, dynamic reserve with 50%–5% quantile
DUC-DR-1	Deterministic UC with deterministic forecast, dynamic reserve with 50%–1% quantile
DUC-DZR-40	Deterministic UC with deterministic forecast, dynamic reserve with 50%–40% quantile, zonal implementation
DUC-DZR-30	Deterministic UC with deterministic forecast, dynamic reserve with 50%–30% quantile, zonal implementation
DUC-DZR-20	Deterministic UC with deterministic forecast, dynamic reserve with 50%–20% quantile, zonal implementation
DUC-DZR-10	Deterministic UC with deterministic forecast, dynamic reserve with 50%–10% quantile, zonal implementation
DUC-DZR-5	Deterministic UC with deterministic forecast, dynamic reserve with 50%–5% quantile, zonal implementation
DUC-DZR-1	Deterministic UC with deterministic forecast, dynamic reserve with 50%–1% quantile, zonal implementation
IUC-40	Interval UC with 40% quantile LB
IUC-30	Interval UC with 30% quantile LB
IUC-20	Interval UC with 20% quantile LB
IUC-10	Interval UC with 10% quantile LB
IUC-5	Interval UC with 5% quantile LB
IUC-1	Interval UC with 1% quantile LB
SUC-E-0	Extensive-form stochastic UC with 10 scenarios and no additional reserve derived from wind scenario
SUC-E-1	Extensive-form stochastic UC with 10 scenarios and 1% additional scenario reserve
SUC-E-5	Extensive-form stochastic UC with 10 scenarios and 5% additional scenario reserve
SUC-E-10	Extensive-form stochastic UC with 10 scenarios and 10% additional scenario reserve
SUC-EZ-1	Extensive-form stochastic UC with 10 scenarios and 1% additional scenario reserve, zonal implementation
SUC-EZ-5	Extensive-form stochastic UC with 10 scenarios and 5% additional scenario reserve, zonal implementation
SUC-EZ-10	Extensive-form stochastic UC with 10 scenarios and 10% additional scenario reserve, zonal implementation
SUC-L-0	LSF decomposition stochastic UC with 10 scenarios
SUC-L-1	LSF decomposition stochastic UC with 10 scenarios and 1% additional scenario reserve
SUC-L-5	LSF decomposition stochastic UC with 10 scenarios and 5% additional scenario reserve
SUC-L-10	LSF decomposition stochastic UC with 10 scenarios and 10% additional scenario reserve

TABLE 2 (Cont.)

Case Number	Description
SUC-LZ-1	LSF decomposition stochastic UC with 10 scenarios and 1% additional scenario reserve, zonal implementation
SUC-LZ-5	LSF decomposition stochastic UC with 10 scenarios and 5% additional scenario reserve, zonal implementation
SUC-LZ-10	LSF decomposition stochastic UC with 10 scenarios and 10% additional scenario reserve, zonal implementation
SUC-B-0	BD stochastic UC with 10 scenarios
SUC-B-1	BD stochastic UC with 10 scenarios and 1% additional scenario reserve
SUC-B-5	BD stochastic UC with 10 scenarios and 5% additional scenario reserve
SUC-B-10	BD stochastic UC with 10 scenarios and 10% additional scenario reserve
SUC-BZ-1	BD stochastic UC with 10 scenarios and 1% additional scenario reserve, zonal implementation
SUC-BZ-5	BD stochastic UC with 10 scenarios and 5% additional scenario reserve, zonal implementation
SUC-BZ-10	BD stochastic UC with 10 scenarios and 10% additional scenario reserve, zonal implementation

TABLE 3 Summer Average Daily Day-ahead Total Cost

Case Number	Cost (10^6 \$)	Case Number	Cost (10^6 \$)	Case Number	Cost (10^6 \$)
DUC-perfect	1.5174				
DUC-point	1.5892				
DUC-DR-40	1.6021	DUC-DRZ-40	1.6022	IUC-40	1.5912
DUC-DR-30	1.6138	DUC-DRZ-30	1.6140	IUC-30	1.5978
DUC-DR-20	1.6252	DUC-DRZ-20	1.6357	IUC-20	1.6073
DUC-DR-10	1.6374	DUC-DRZ-10	1.7761	IUC-10	1.6234
DUC-DR-5	1.6470	DUC-DRZ-5	1.9733	IUC-5	1.6357
DUC-DR-1	1.6813	DUC-DRZ-1	2.2414	IUC-1	1.6463
SUC-E-0	1.5646	SUC-L-0	1.5647	SUC-B-0	1.5720
SUC-E-1	1.5653	SUC-L-1	1.5654	SUC-B-1	1.5725
SUC-E-5	1.5679	SUC-L-5	1.5681	SUC-B-5	1.5746
SUC-E-10	1.5714	SUC-L-10	1.5714	SUC-B-10	1.5790
SUC-EZ-1	1.5653	SUC-LZ-1	1.5654	SUC-BZ-1	1.5716
SUC-EZ-5	1.5680	SUC-LZ-5	1.5681	SUC-BZ-5	1.5753
SUC-EZ-10	1.5714	SUC-LZ-10	1.5714	SUC-BZ-10	1.5787

TABLE 4 Summer Average Daily Day-ahead Total Energy Cost

Case Number	Cost (10^6 \$)	Case Number	Cost (10^6 \$)	Case Number	Cost (10^6 \$)
DUC-perfect	1.5011				
DUC-point	1.5729				
DUC-DR-40	1.5729	DUC-DRZ-40	1.5730	IUC-40	1.5727
DUC-DR-30	1.5732	DUC-DRZ-30	1.5732	IUC-30	1.5729
DUC-DR-20	1.5736	DUC-DRZ-20	1.5758	IUC-20	1.5751
DUC-DR-10	1.5752	DUC-DRZ-10	1.5817	IUC-10	1.5809
DUC-DR-5	1.5777	DUC-DRZ-5	1.5869	IUC-5	1.5872
DUC-DR-1	1.5811	DUC-DRZ-1	1.5918	IUC-1	1.5938
SUC-E-0	1.5483	SUC-L-0	1.5484	SUC-B-0	1.5557
SUC-E-1	1.5483	SUC-L-1	1.5484	SUC-B-1	1.5556
SUC-E-5	1.5483	SUC-L-5	1.5484	SUC-B-5	1.5549
SUC-E-10	1.5483	SUC-L-10	1.5484	SUC-B-10	1.5560
SUC-EZ-1	1.5483	SUC-LZ-1	1.5484	SUC-BZ-1	1.5546
SUC-EZ-5	1.5483	SUC-LZ-5	1.5485	SUC-BZ-5	1.5556
SUC-EZ-10	1.5483	SUC-LZ-10	1.5484	SUC-BZ-10	1.5555

TABLE 5 Fall Average Daily Day-ahead Total Cost

Case Number	Cost (10^6 \$)	Case Number	Cost (10^6 \$)	Case Number	Cost (10^6 \$)
DUC-perfect	1.0235				
DUC-point	1.0744				
DUC-DR-40	1.0897	DUC-DRZ-40	1.0902	IUC-40	1.0776
DUC-DR-30	1.1053	DUC-DRZ-30	1.1091	IUC-30	1.0865
DUC-DR-20	1.1226	DUC-DRZ-20	1.1568	IUC-20	1.1031
DUC-DR-10	1.1461	DUC-DRZ-10	1.3760	IUC-10	1.1313
DUC-DR-5	1.1655	DUC-DRZ-5	1.6880	IUC-5	1.1486
DUC-DR-1	1.2890	DUC-DRZ-1	2.1998	IUC-1	1.1679
SUC-E-0	1.0779	SUC-L-0	1.0739	SUC-B-0	1.0776
SUC-E-1	1.0750	SUC-L-1	1.0749	SUC-B-1	1.0786
SUC-E-5	1.0787	SUC-L-5	1.0785	SUC-B-5	1.0846
SUC-E-10	1.0832	SUC-L-10	1.0830	SUC-B-10	1.0869
SUC-EZ-1	1.0749	SUC-LZ-1	1.0748	SUC-BZ-1	1.0812
SUC-EZ-5	1.0788	SUC-LZ-5	1.0787	SUC-BZ-5	1.0827
SUC-EZ-10	1.0839	SUC-LZ-10	1.0836	SUC-BZ-10	1.0875

TABLE 6 Fall Average Daily Day-ahead Energy Cost

Case Number	Cost (10^6 \$)	Case Number	Cost (10^6 \$)	Case Number	Cost (10^6 \$)
DUC-perfect	1.0072				
DUC-point	1.0582				
DUC-DR-40	1.0585	DUC-DRZ-40	1.0591	IUC-40	1.0583
DUC-DR-30	1.0595	DUC-DRZ-30	1.0620	IUC-30	1.0587
DUC-DR-20	1.0622	DUC-DRZ-20	1.0702	IUC-20	1.0642
DUC-DR-10	1.0704	DUC-DRZ-10	1.0858	IUC-10	1.0784
DUC-DR-5	1.0796	DUC-DRZ-5	1.0968	IUC-5	1.0895
DUC-DR-1	1.0956	DUC-DRZ-1	1.1130	IUC-1	1.1034
SUC-E-0	1.0616	SUC-L-0	1.0577	SUC-B-0	1.0613
SUC-E-1	1.0578	SUC-L-1	1.0577	SUC-B-1	1.0615
SUC-E-5	1.0580	SUC-L-5	1.0578	SUC-B-5	1.0639
SUC-E-10	1.0580	SUC-L-10	1.0578	SUC-B-10	1.0617
SUC-EZ-1	1.0578	SUC-LZ-1	1.0576	SUC-BZ-1	1.0640
SUC-EZ-5	1.0581	SUC-LZ-5	1.0579	SUC-BZ-5	1.0619
SUC-EZ-10	1.0587	SUC-LZ-10	1.0584	SUC-BZ-10	1.0622

As we increase the dynamic reserve requirements for DUC or consider a lower interval bound for IUC, the system improves its reliability with a higher energy and reserve cost. The zonal reserve demands the same amount of dynamic reserve with a stricter rule about its locational deployment. Therefore, it always costs more than its DUC-DR counterpart. When DUC hedges for a larger wind uncertainty range, the increased cost is due in part to a large reserve penalty cost, as will be shown later. It appears that the increased reliability does not yield enough overall system benefits, measured in terms of costs.

Similarly, IUC cost increases as a lower-quantile corrective transition security is ensured. Compared to DUC, this cost increment is not as significant. In addition, the IUC produces a lower total cost than DUC with the same LB optimized, even though the schedule cost (energy cost) is higher in most cases. Note that IUC always reaches a more reliable schedule (less or no load shedding) compared to DUC with the same LB. This is because the additional LB constraints in IUC ensure the system feasibility (power balance, reserve balance, transmission line constraints) in those defined worst cases.

For SUC, as extensive-form and LSF decomposition have almost identical formulations, their costs are very close to each other and within the optimality gap. The small amounts of additional explicit dynamic reserve do not affect schedule cost much under SUC, which means that the commitment status does not change much with the small amounts of additional reserves. In addition, this schedule is more economical than DUC and IUC in both summer and fall. SUC strategies can be even cheaper than DUC-point strategies when strong wind is present in the fall. For the BD SUC, as we adopt a slightly larger MIP gap to solve each master problem, the final solution obtained is slightly more expensive than for LSF and extensive-form decomposition.

With a smaller MIP gap, the solution can be improved and will be closer to the LSF solutions at the cost of a larger computing time, which reduces the computational benefit from BD.

Note that the SUC and IUC approaches both schedule wind reserves implicitly. In contrast, the DUC strategy schedules explicit reserves for wind power through the reserve constraints. There is, therefore, a direct cost, reflected in the objective function and in the total costs reported in Table 3, of these wind reserves under DUC. The cost of additional implicit wind reserves in the IUC formulation is also accounted for, but in the SUC formulation there is no explicit cost for the implicit reserves. Hence, care must be taken when comparing the DA total cost results, as DUC and IUC results reflect a cost element for wind reserves that is not reflected for SUC. The reported total energy cost figures are more directly comparable, as they do not include the cost of reserves. Still, note that the SUC strategy finds the expected DA cost over multiple wind scenarios, as opposed to the DUC and IUC strategies that optimize for the default point forecast scenario only.

5.2.2 Real-time Costs

In the RT simulations, all cases impose the same reserve requirements, which are limited to the amount needed for contingency reserves. Moreover, since there are no RT contingency reserve curtailments and corresponding penalties in any of the cases, the reserve cost is the same for all cases. Therefore, in TABLE 7 and TABLE 8 we only present the total cost results for the RT stage. The results indicate that in the summer, the net load is relatively large, more generators are therefore on, and online capacity is sufficient to mitigate the forecast inaccuracy from DA scheduling to RT-ED. In this case, when the system buys more explicit reserve as in DUC-DR and schedules more implicit reserve in IUC, the additional cost from this reserve component does not yield economic benefits. In contrast, when the net load is relatively lower in the fall, online capacity is not enough to handle the extreme events without additional reserves, and load shedding occurs on particular days in the DUC-point case. In these cases, dynamic reserve and IUC produce a more reliable schedule, and the additional reserves from the DA and RAC stages result in cost savings because of lower load curtailment.

In sensitivity runs, when we choose a more conservative strategy and select a lower quantile, such as 5% or 1%, the reliability for IUC holds, and for dynamic reserves the RT load shedding is reduced. However, as we compare the cost components, DUC with dynamic reserve pays more for buying reserves in the DA stage from slow generators and produces a cheaper schedule in the RT stage. In contrast, IUC provides more implicit reserves from quick-start units in the DA stage with less reserve bought, but the IUC schedule is more expensive in RT stages. On the contrary, when we choose a less conservative strategy and select a higher quantile of 20% or 30%, the reliability for IUC also decreases, and DUC can reach a point where the purchased dynamic reserve is economically viable to compensate for the possible load-shedding penalty. The results show that the 20% LB yields the lowest RT cost in the high-wind/low-load fall season for both DUC and IUC. This result suggests that optimizing the dynamic reserve amount in DUC or the lower interval bound under IUC can find a good balance between economics and reliability. This is a promising direction for future research.

TABLE 7 Summer Average Daily Real-time Total Cost

Case Number	Cost (10^6 \$)	Case Number	Cost (10^6 \$)	Case Number	Cost (10^6 \$)
DUC-perfect	1.5174				
DUC-point	1.5228				
DUC-DR-40	1.5231	DUC-DRZ-40	1.5230	IUC-40	1.5227
DUC-DR-30	1.5231	DUC-DRZ-30	1.5230	IUC-30	1.5227
DUC-DR-20	1.5229	DUC-DRZ-20	1.5245	IUC-20	1.5232
DUC-DR-10	1.5232	DUC-DRZ-10	1.5281	IUC-10	1.5244
DUC-DR-5	1.5246	DUC-DRZ-5	1.5330	IUC-5	1.5274
DUC-DR-1	1.5275	DUC-DRZ-1	1.5370	IUC-1	1.5317
SUC-E-0	1.5209	SUC-L-0	1.5209	SUC-B-0	1.5279
SUC-E-1	1.5209	SUC-L-1	1.5210	SUC-B-1	1.5281
SUC-E-5	1.5209	SUC-L-5	1.5210	SUC-B-5	1.5281
SUC-E-10	1.5210	SUC-L-10	1.5209	SUC-B-10	1.5285
SUC-EZ-1	1.5209	SUC-LZ-1	1.5209	SUC-BZ-1	1.5271
SUC-EZ-5	1.5209	SUC-LZ-5	1.5209	SUC-BZ-5	1.5281
SUC-EZ-10	1.5209	SUC-LZ-10	1.5209	SUC-BZ-10	1.5280

TABLE 8 Fall Average Daily Real-time Total Cost

Case Number	Cost (10^6 \$)	Case Number	Cost (10^6 \$)	Case Number	Cost (10^6 \$)
DUC-perfect	1.0235				
DUC-point	1.0498				
DUC-DR-40	1.0495	DUC-DRZ-40	1.0533	IUC-40	1.0444
DUC-DR-30	1.0449	DUC-DRZ-30	1.0441	IUC-30	1.0416
DUC-DR-20	1.0397	DUC-DRZ-20	1.0458	IUC-20	1.0407
DUC-DR-10	1.0432	DUC-DRZ-10	1.0566	IUC-10	1.0464
DUC-DR-5	1.0473	DUC-DRZ-5	1.0643	IUC-5	1.0520
DUC-DR-1	1.0573	DUC-DRZ-1	1.0743	IUC-1	1.0585
SUC-E-0	1.0338	SUC-L-0	1.0336	SUC-B-0	1.0384
SUC-E-1	1.0336	SUC-L-1	1.0337	SUC-B-1	1.0375
SUC-E-5	1.0340	SUC-L-5	1.0338	SUC-B-5	1.0387
SUC-E-10	1.0336	SUC-L-10	1.0336	SUC-B-10	1.0370
SUC-EZ-1	1.0336	SUC-LZ-1	1.0336	SUC-BZ-1	1.0425
SUC-EZ-5	1.0339	SUC-LZ-5	1.0342	SUC-BZ-5	1.0362
SUC-EZ-10	1.0340	SUC-LZ-10	1.0338	SUC-BZ-10	1.0369

For SUC cases, the scenarios capture the wind uncertainty better. In the DA-UC stage, SUC encourages more flexible units (including quick-start units and slow-start units with large ramping capabilities) online, and the wind utilization rate is higher with less wind spillage, resulting in a similar range of DA costs compared to DUC-point. As the wind uncertainty is better managed with SUC, all the SUC RT-ED solutions are very close to the DUC-perfect case and cheaper than the other DUC and IUC cases, for both summer and fall. At the same time, there is no load shedding at all, showing that the optimized schedule is also reliable. Hence, the results indicate that SUC reaches a better balance between system costs and reliability.

Note, again, that in the RT stage, all the strategies impose the same reserve requirements, i.e. contingency reserves only, and also solve for only one wind scenario, i.e., the realized availability for wind power. Hence, the RT total cost results in TABLE 7 and TABLE 8 can be directly compared across the cases.

5.3 RESERVE COSTS

Tables 9 and 10 present total DA reserve costs, which include reserve purchase costs and reserve curtailment penalty costs. The reserve purchase cost is the largest cost element in most cases. However, when we impose a strict reserve policy, especially in the high-wind fall season, reserve curtailment drives the reserve costs to a large value, especially in the zonal cases. The results demonstrate that it is important to properly select the reserve rules to balance the need for system reliability with the additional costs of scheduling more reserves. For DUC, the reserve costs increase with an increase in the reserve requirements (i.e., lower forecast quantile). Moreover, imposing zonal reserve requirements increases the reserve cost, particularly for high reserve levels. The IUC cases have lower reserve costs than DUC, indicating that the reserves are scheduled more efficiently with the implicit IUC reserve strategy. SUC cases have the lowest reserve costs, since the cost of implicit wind reserves are not considered under this formulation, i.e., only the cost of contingency reserves are accounted for explicitly in the base SUC-E-0 case. Note that the other SUC cases do also purchase additional explicit reserves in each wind scenario, but these reserve levels and costs are small compared to the dynamic wind reserves in the DUC cases.

5.4 CURTAILMENT OF RESERVE AND LOAD

5.4.1 Day-ahead

From Tables 11 and 12, we observe that the DA load-shedding amount is very limited. As there is a $ 3500/MWh load-shedding penalty, the UC optimizes the schedule to minimize this penalty payment. For the DUC and IUC cases, this payment is entirely avoided by adopting a more expensive schedule. For the SUC cases, as multiple scenarios are considered, load shedding occurs for some particular scenarios on certain days, primarily in the fall. This load-shedding penalty may be tolerable from an economic perspective, as we see that the total cost is still lower for the SUC cases.

TABLE 9 Summer Average Daily Day-ahead Reserve Cost

Case Number	Cost (10^6 \$)	Case Number	Cost (10^6 \$)	Case Number	Cost (10^6 \$)
DUC-perfect	0.0163				
DUC-point	0.0163				
DUC-DR-40	0.0292	DUC-DRZ-40	0.0292	IUC-40	0.0185
DUC-DR-30	0.0407	DUC-DRZ-30	0.0408	IUC-30	0.0249
DUC-DR-20	0.0516	DUC-DRZ-20	0.0599	IUC-20	0.0322
DUC-DR-10	0.0621	DUC-DRZ-10	0.1945	IUC-10	0.0425
DUC-DR-5	0.0693	DUC-DRZ-5	0.3864	IUC-5	0.0485
DUC-DR-1	0.1002	DUC-DRZ-1	0.6496	IUC-1	0.0525
SUC-E-0	0.0163	SUC-L-0	0.0163	SUC-B-0	0.0163
SUC-E-1	0.0170	SUC-L-1	0.0170	SUC-B-1	0.0169
SUC-E-5	0.0197	SUC-L-5	0.0196	SUC-B-5	0.0196
SUC-E-10	0.0230	SUC-L-10	0.0230	SUC-B-10	0.0230
SUC-EZ-1	0.0170	SUC-LZ-1	0.0170	SUC-BZ-1	0.0170
SUC-EZ-5	0.0197	SUC-LZ-5	0.0196	SUC-BZ-5	0.0196
SUC-EZ-10	0.0230	SUC-LZ-10	0.0230	SUC-BZ-10	0.0232

TABLE 10 Fall Average Daily Day-ahead Reserve Cost

Case Number	Cost (10^6 \$)	Case Number	Cost (10^6 \$)	Case Number	Cost (10^6 \$)
DUC-perfect	0.0163				
DUC-point	0.0163				
DUC-DR-40	0.0311	DUC-DRZ-40	0.0311	IUC-40	0.0192
DUC-DR-30	0.0458	DUC-DRZ-30	0.0471	IUC-30	0.0278
DUC-DR-20	0.0604	DUC-DRZ-20	0.0866	IUC-20	0.0389
DUC-DR-10	0.0757	DUC-DRZ-10	0.2902	IUC-10	0.0529
DUC-DR-5	0.0859	DUC-DRZ-5	0.5912	IUC-5	0.0591
DUC-DR-1	0.1934	DUC-DRZ-1	1.0868	IUC-1	0.0645
SUC-E-0	0.0163	SUC-L-0	0.0163	SUC-B-0	0.0163
SUC-E-1	0.0172	SUC-L-1	0.0172	SUC-B-1	0.0172
SUC-E-5	0.0207	SUC-L-5	0.0207	SUC-B-5	0.0207
SUC-E-10	0.0252	SUC-L-10	0.0252	SUC-B-10	0.0252
SUC-EZ-1	0.0172	SUC-LZ-1	0.0172	SUC-BZ-1	0.0172
SUC-EZ-5	0.0207	SUC-LZ-5	0.0207	SUC-BZ-5	0.0207
SUC-EZ-10	0.0252	SUC-LZ-10	0.0252	SUC-BZ-10	0.0252

TABLE 11 Summer Daily Average Day-ahead Load Shedding Amount

Case Number	MW	Case Number	MW	Case Number	MW
DUC-perfect	0				
DUC-point	0				
DUC-DR-40	0	DUC-DRZ-40	0	IUC-40	0
DUC-DR-30	0	DUC-DRZ-30	0	IUC-30	0
DUC-DR-20	0	DUC-DRZ-20	0	IUC-20	0
DUC-DR-10	0	DUC-DRZ-10	0	IUC-10	0
DUC-DR-5	0	DUC-DRZ-5	0	IUC-5	0
DUC-DR-1	0	DUC-DRZ-1	0	IUC-1	0
SUC-E-0	0	SUC-L-0	0	SUC-B-0	0
SUC-E-1	0	SUC-L-1	0	SUC-B-1	0
SUC-E-5	0	SUC-L-5	0	SUC-B-5	0
SUC-E-10	0	SUC-L-10	0	SUC-B-10	0
SUC-EZ-1	0	SUC-LZ-1	0	SUC-BZ-1	0
SUC-EZ-5	0	SUC-LZ-5	0	SUC-BZ-5	0
SUC-EZ-10	0	SUC-LZ-10	0	SUC-BZ-10	0.0102

TABLE 12 Fall Daily Average Day-ahead Load Shedding Amount

Case Number	MW	Case Number	MW	Case Number	MW
DUC-perfect	0				
DUC-point	0				
DUC-DR-40	0	DUC-DRZ-40	0	IUC-40	0
DUC-DR-30	0	DUC-DRZ-30	0	IUC-30	0
DUC-DR-20	0	DUC-DRZ-20	0	IUC-20	0
DUC-DR-10	0	DUC-DRZ-10	0	IUC-10	0
DUC-DR-5	0	DUC-DRZ-5	0	IUC-5	0
DUC-DR-1	0	DUC-DRZ-1	0	IUC-1	0
SUC-E-0	1.0756	SUC-L-0	0	SUC-B-0	0.0251
SUC-E-1	0.0036	SUC-L-1	0	SUC-B-1	0.1200
SUC-E-5	0.0039	SUC-L-5	0.0002	SUC-B-5	0.8666
SUC-E-10	0	SUC-L-10	0	SUC-B-10	0.2418
SUC-EZ-1	0	SUC-LZ-1	0	SUC-BZ-1	0.7598
SUC-EZ-5	0	SUC-LZ-5	0	SUC-BZ-5	0.2951
SUC-EZ-10	0.0033	SUC-LZ-10	0	SUC-BZ-10	0.1475

Tables 13 to 15 show that the reserve curtailment mainly occurs for the DUC with zonal reserves. With larger reserve requirements, there tends to be a larger reserve penalty, as the system cannot always provide such reserve amounts and has to curtail certain amounts even if doing so is very expensive. Table 15 further presents the curtailment for the different reserve products, averaged across the four months. Spinning reserve suffers from the most curtailment, which is not surprising, since the reserve-shedding penalties follow the order of non-spinning, which corresponds to total reserve ($1100/MWh), regulation ($1000/MWh), and spinning ($850/MWh) [8] [46]. Hence, the system curtails spinning reserves, the cheapest products, first. To avoid load shedding, which has a higher penalty, non-spinning reserve curtailment is sometimes implemented during periods of high reserve requirements. From Tables 13–15, we observe that the dynamic reserve requirement should be properly selected, and a too large value would decrease the economic benefit without improving reliability.

TABLE 13 Summer Average Daily Day-ahead Reserve Curtailment

Case Number	MW	Case Number	MW	Case Number	MW
DUC-perfect	0				
DUC-point	0				
DUC-DR-40	0	DUC-DRZ-40	0	IUC-40	0
DUC-DR-30	0	DUC-DRZ-30	0.0001	IUC-30	0
DUC-DR-20	0	DUC-DRZ-20	0.0083	IUC-20	0
DUC-DR-10	0	DUC-DRZ-10	0.1323	IUC-10	0
DUC-DR-5	0.0013	DUC-DRZ-5	0.3184	IUC-5	0
DUC-DR-1	0.0279	DUC-DRZ-1	0.5773	IUC-1	0
SUC-E-0	0	SUC-L-0	0	SUC-B-0	0
SUC-E-1	0	SUC-L-1	0	SUC-B-1	0
SUC-E-5	0	SUC-L-5	0	SUC-B-5	0
SUC-E-10	0	SUC-L-10	0	SUC-B-10	0
SUC-EZ-1	0	SUC-LZ-1	0	SUC-BZ-1	0
SUC-EZ-5	0	SUC-LZ-5	0	SUC-BZ-5	0
SUC-EZ-10	0	SUC-LZ-10	0	SUC-BZ-10	0.0002

TABLE 14 Fall Average Daily Day-ahead Reserve Curtailment

Case Number	MW	Case Number	MW	Case Number	MW
DUC-perfect	0				
DUC-point	0				
DUC-DR-40	0	DUC-DRZ-40	0	IUC-40	0
DUC-DR-30	0	DUC-DRZ-30	0.0013	IUC-30	0
DUC-DR-20	0	DUC-DRZ-20	0.0262	IUC-20	0
DUC-DR-10	0	DUC-DRZ-10	0.2146	IUC-10	0
DUC-DR-5	0.0024	DUC-DRZ-5	0.5077	IUC-5	0
DUC-DR-1	0.1021	DUC-DRZ-1	0.9957	IUC-1	0
SUC-E-0	0	SUC-L-0	0	SUC-B-0	0
SUC-E-1	0	SUC-L-1	0	SUC-B-1	0
SUC-E-5	0	SUC-L-5	0	SUC-B-5	0
SUC-E-10	0	SUC-L-10	0	SUC-B-10	0
SUC-EZ-1	0	SUC-LZ-1	0	SUC-BZ-1	0
SUC-EZ-5	0	SUC-LZ-5	0	SUC-BZ-5	0
SUC-EZ-10	0.0001	SUC-LZ-10	0.0001	SUC-BZ-10	0.0001

TABLE 15 Four-Month Average Daily Day-ahead Reserve Curtailment for DUC Cases

Case Number	Regulation Up (MW)	Regulation Down (MW)	Spinning (MW)	Non-Spinning (MW)
DUC-DR-40	0	0	0	0
DUC-DR-30	0.0005	0.0005	0.0033	0
DUC-DR-20	0	0	0.0072	0
DUC-DR-10	0	0	0.0093	0
DUC-DR-5	0	0.5990	1.4641	0
DUC-DR-1	0.8841	7.250	26.6372	30.87
DUC-DRZ-40	0	0	0	0
DUC-DRZ-30	0	0	0.0032	0
DUC-DRZ-20	0	0	0.0072	0
DUC-DRZ-10	0	0	0.0275	0
DUC-DRZ-5	0	0.7337	1.3047	0.4935
DUC-DRZ-1	0.7430	7.056	27.33	30.90

5.4.2 Real-time

Table 16 presents the RT load shedding results for the fall. As the wind power generation is relatively low in summer, there is no load shedding at all. However, as wind availability is higher in the fall, the forecast inaccuracy brings more challenges to the system, and there is load shedding for DUC cases on some particular days with poor wind power forecasts. Although dynamic reserves and also zonal settings provide room to hedge against the forecast errors, these strategies still cannot mitigate the error as well as in the SUC cases. Even though BD solutions are not as good as the other two SUC solution methods, they are still better than the DUC cases in terms of load shedding. Since the worst-case wind is considered, IUC also performs well here when the LB is based on lower quantiles.

There is no reserve curtailment in RT dispatch, as we only impose a system-wide contingency reserve requirement in the RT dispatch simulation. This contingency reserve amount is not large and is easy to cope with for all the scheduling approaches.

TABLE 16 Fall Average Daily Real-time Load Shedding

Case Number	MW	Case Number	MW	Case Number	MW
DUC-perfect	0				
DUC-point	3.4257				
DUC-DR-40	3.3233	DUC-DRZ-40	4.4695	IUC-40	1.8495
DUC-DR-30	2.0674	DUC-DRZ-30	1.2941	IUC-30	1.0830
DUC-DR-20	0.4593	DUC-DRZ-20	0.1167	IUC-20	0.3307
DUC-DR-10	0.5161	DUC-DRZ-10	0	IUC-10	0
DUC-DR-5	0.2856	DUC-DRZ-5	0	IUC-5	0
DUC-DR-1	0	DUC-DRZ-1	0	IUC-1	0
SUC-E-0	0	SUC-L-0	0	SUC-B-0	0.2056
SUC-E-1	0	SUC-L-1	0	SUC-B-1	0.2126
SUC-E-5	0	SUC-L-5	0	SUC-B-5	0.6239
SUC-E-10	0	SUC-L-10	0	SUC-B-10	0
SUC-EZ-1	0	SUC-LZ-1	0	SUC-BZ-1	1.3849
SUC-EZ-5	0	SUC-LZ-5	0	SUC-BZ-5	0
SUC-EZ-10	0	SUC-LZ-10	0	SUC-BZ-10	0

5.5 WIND CURTAILMENT

Different wind profiles and representations are used for the different formulations at the DA stage. In contrast, at the RT stage, every formulation uses the same realized wind data. Therefore, RT-stage wind curtailment is a good illustration of the system wind utilization level. In Table 17, we present the average daily total wind curtailments for summer and fall in RT. Not surprisingly, the perfect-forecast case results in the lowest wind curtailment, as the scheduling is based on perfect foresight of available wind power. Among the other cases, SUC performs the best in terms of reducing the wind curtailment, indicating that the scenarios capture the uncertainty quite well and schedule resources accordingly. DUC is worse than SUC but better than IUC. IUC curtails the most wind to ensure feasible operation in preparation for the worst-case scenario. In general, higher explicit or implicit reserves in DUC and SUC, respectively, give rise to slightly more wind curtailments as additional units are scheduled to provide reserves, as discussed in the next section.

5.6 NUMBER OF COMMITMENTS

In Table 18, we present the average daily number of commitments for fast (i.e., oil and gas) and slow (i.e., coal) generators. As the two reference DUC strategies (perfect and point) rely on a point forecast only, they tend to use the cheaper slow units as much as possible. In contrast, the dynamic reserve and IUC cases consider the wind-power forecast uncertainty and more quick-start units are running for these cases, especially for lower forecast quantiles. As IUC provides implicit reserve and ensures the reserve deliverability for the transition and LB forecast

TABLE 17 Average Daily Total Real-time Wind Curtailments

	Wind Curtailments (MWh)	
Case Number	Summer	Fall
DUC-perfect	540	1361
DUC-point	732	2199
DUC-DR -30	737	2214
DUC-DR -10	735	2239
DUC-DRZ-30	733	2158
DUC-DRZ-10	751	2287
IUC-30	737	2224
IUC-10	783	2551
SUC-E-0	712	2044
SUC-E-5	711	2044
SUC-EZ-5	712	2030

cases, the IUC cases tend to start up more quick-start units with a more expensive schedule. For the same forecast interval, DUC starts fewer generators than DUC-Z, while IUC starts more units than DUC-Z.

The results also show that the stochastic cases commit significantly fewer units to hedge against uncertainty. The advantage of SUC is evident, as it commits fewer units at the DA and RAC stages than DUC and IUC but with better reliability. Therefore, the results indicate that a stochastic formulation with a good representation of uncertainty can reduce unnecessary start-ups.

Additional quick-start units can be started in RAC when necessary. For the less-windy summer season, Table 18 shows that there are only small changes in the average commitment levels between DA and RAC, indicating that the need for doing re-commitments in RAC is limited. The differences are somewhat more significant in the more windy fall season, i.e., with more adjustments in RAC. Note that the SUC cases tend to give smaller changes in commitments between DA and RAC than the DUC and IUC cases, indicating that the DA schedule under SUC is more capable of handling deviations in the wind power forecast. Different reserve strategies do not significantly change the commitment decisions under SUC. Therefore, their operational schedules are close to the two reference cases (DUC-perfect and DUC-point) and still have better reliability metrics than other operational strategies (Table 16). Hence, Tables 16–18 illustrate the advantage of stochastic scheduling methods. Table 18 shows that the DUC and IUC strategies schedule more units than SUC, particularly in the fall season. Furthermore, more units are scheduled with increasing reserve requirements. Finally, zonal reserves tend to increase the number of commitments under DUC.

TABLE 18 Average Daily Number of Commitments

	Summer					Fall				
		Fast Units		Total Units			Fast Units		Total Units	
Case Number	Slow Units	DA	RAC	DA	RAC	Slow Units	DA	RAC	DA	RAC
DUC-perfect	705.7	0.6	0.6	706.3	706.3	564.8	1.5	1.5	566.3	566.3
DUC-point	728.7	1.5	1.3	730.2	730.0	597.4	0.8	1.7	598.2	599.1
DUC-DR -30	725.6	2.5	2.1	728.1	727.7	594.0	0.9	2.1	594.9	596.1
DUC-DR -10	732.5	5.3	3.9	737.8	736.4	626.1	20.5	17.8	646.6	643.9
DUC-DRZ-30	727.2	3.0	2.4	730.2	729.6	600.4	4.1	8.0	604.5	608.4
DUC-DRZ-10	735.5	13.0	9.1	748.5	744.6	639.8	33.0	42.4	672.8	682.2
IUC-30	732.3	2.5	2.5	734.8	734.8	610.5	0.9	2.7	611.4	613.2
IUC-10	760.7	22.9	17.0	783.6	777.7	706.4	30.4	26.1	736.8	732.5
SUC-E-0	711.0	3.5	3.4	714.5	714.4	567.4	1.0	3.3	568.4	570.7
SUC-E-5	710.8	3.5	3.3	714.3	714.1	566.5	1.5	3.4	568.0	569.9
SUC-EZ-5	710.8	3.5	3.2	714.3	714.0	566.3	1.6	3.3	567.9	569.6

5.7 COMPUTATION

The computational effort is also a very important metric when comparing different scheduling strategies. The computational wall-clock time is shown in Tables 19 and 20. Compared to DUC-point, procuring additional dynamic reserves increases the computing time, but the overall speed is still fast. As the reserve requirement increases, the problem becomes much harder to solve. Note that there is a substantial difference between DUC-DR-10 and DUC-DR-5. DUC-Z has similar performance characteristics to DUC, but is slightly slower.

Interestingly, IUC outperforms DUC from a computational perspective, and performs very similarly to the two DUC reference cases. The reason is that IUC adds a set of feasibility check constraints to ensure that the system has enough reserve, and these constraints drive the system to schedule implicit reserve only when it is necessary, sometimes resulting in less reserves scheduled compared to the DUC case. Therefore, IUC adds less computational burden than the dynamic reserve case. Another interesting finding is that the lower quantile even drives the program to be faster. This is probably because with a lower quantile, the feasible region can be more efficiently solved by CPLEX.

As expected, the computation time is significantly longer for the SUC cases compared to IUC and DUC. Still, with ten scenarios, the average times are all below 10 minutes for the DA problem. Note that although the extensive-form formulation has similar computing times to the LSF decomposition, there are out-of-memory issues for particular days where CPLEX fails to provide a solution. Hence, the optimality gap and other settings have to be relaxed and adjusted to provide a solution. BD is faster than the extensive-form formulation and the LSF decomposition, especially at the RAC stage (Table 20), but some efforts are needed to construct proper subproblems for better convergence. With the current 1% MIP gap, the solution is not as good as the extensive-form and LSF solutions. When experimenting with a lower gap, such as 0.5% or even 0.1%, the bloating master problem quickly makes this problem intractable and it takes a much longer time to solve and converge. In contrast, with LSF decomposition, these extra manual tuning efforts are not necessary. In general, decomposition enables one to consistently find solutions for cases incorporating more scenarios. Increasing the number of scenarios is something we plan to test in future work.

Table 21 shows that LSF decomposition generally converges in 4 iterations. Each cut is essentially representing one congested or potentially congested line. On average, only 0.73% of the lines are potentially congested for case SUC-L-0. These convergence statistics do not change much as we change the dynamic reserve settings. A better initialization step could place pre-defined critical lines in the line checking set to further reduce the computing time. This approach could save time, as fewer iterations of solving the repeated master MIP problem would be necessary.

Finally, Table 22 also shows that BD can normally converge in 16–20 iterations to reach the optimality criterion for the DA problem. However, for some extreme cases, the maximum iteration limit of 100 is met. In contrast, after fixing the slow generators, RAC only needs one more iteration to find the optimal solution. With a lower MIP gap for the master problem, it would take hours or even up to one day. Therefore, we select 1% as the MIP gap for this instance.

TABLE 19 Average Day-ahead Computational Time Per Day (Wall-clock)

Case Number	Time (s)	Case Number	Time (s)	Case Number	Time (s)
DUC-perfect	11.5				
DUC-point	9.6				
DUC-DR-40	8.5	DUC-DRZ-40	10.1	IUC-40	20.8
DUC-DR-30	8.9	DUC-DRZ-30	12.4	IUC-30	16.3
DUC-DR-20	10.7	DUC-DRZ-20	14.7	IUC-20	12.0
DUC-DR-10	22.1	DUC-DRZ-10	22.1	IUC-10	9.7
DUC-DR-5	27.0	DUC-DRZ-5	26.8	IUC-5	14.2
DUC-DR-1	32.9	DUC-DRZ-1	52.1	IUC-1	8.8
SUC-E-0	218.5	SUC-L-0	266.3	SUC-B-0	189.0
SUC-E-1	228.8	SUC-L-1	253.6	SUC-B-1	225.8
SUC-E-5	239.5	SUC-L-5	455.4	SUC-B-5	241.5
SUC-E-10	414.3	SUC-L-10	361.9	SUC-B-10	196.8
SUC-EZ-1	328.1	SUC-LZ-1	349.8	SUC-BZ-1	202.3
SUC-EZ-5	306.4	SUC-LZ-5	468.0	SUC-BZ-5	194.6
SUC-EZ-10	314.9	SUC-LZ-10	762.4	SUC-BZ-10	222.5

TABLE 20 Average RAC Computational Time Per Day

Case Number	Time (s)	Case Number	Time (s)	Case Number	Time (s)
DUC-perfect	4.3				
DUC-point	4.6				
DUC-DR-40	4.4	DUC-DRZ-40	4.5	IUC-40	5.0
DUC-DR-30	4.5	DUC-DRZ-30	4.9	IUC-30	3.9
DUC-DR-20	4.6	DUC-DRZ-20	5.5	IUC-20	4.2
DUC-DR-10	5.9	DUC-DRZ-10	9.4	IUC-10	4.3
DUC-DR-5	25.9	DUC-DRZ-5	9.9	IUC-5	5.7
DUC-DR-1	25.0	DUC-DRZ-1	14.6	IUC-1	4.3
SUC-E-0*	62.1	SUC-L-0	47.7	SUC-B-0	10.7
SUC-E-1*	66.1	SUC-L-1	46.7	SUC-B-1	11.6
SUC-E-5*	67.1	SUC-L-5	57.3	SUC-B-5	10.8
SUC-E-10*	107.5	SUC-L-10	51.6	SUC-B-10	9.6
SUC-EZ-1*	77.0	SUC-LZ-1	54.2	SUC-BZ-1	9.6
SUC-EZ-5*	83.6	SUC-LZ-5	60.0	SUC-BZ-5	9.7
SUC-EZ-10*	78.1	SUC-LZ-10	64.9	SUC-BZ-10	10.1

*Out of memory.

TABLE 21 LSF Decomposition Convergence Statistics

UC Model	DA Average/ Maximum Number of Iterations	DA Average/ Maximum Number of Cuts	RAC Average/ Maximum Number of Iterations	RAC Average/ Maximum Number of Cuts
SUC-L-0	4/7	328/940	3/4	293/702
SUC-L-1	4/6	327/942	3/5	294/701
SUC-L-5	4/6	328/945	3/4	293/680
SUC-L-10	4/6	328/932	3/5	292/700
SUC-LZ-1	4/6	329/948	3/5	292/682
SUC-LZ-5	4/6	329/946	3/4	293/689
SUC-LZ-10	4/7	329/1016	3/5	293/705

TABLE 22 Benders Decomposition Convergence Statistics

UC Model	DA Average/ Maximum Number of Iterations	DA Average/ Maximum Number of Cuts	RAC Average/ Maximum Number of Iterations	RAC Average/ Maximum Number of Cuts
SUC-B-0	16/100	166/1100	2/2	11/11
SUC-B-1	18/100	192/1100	2/2	11/11
SUC-B-5	20/100	208/1100	2/2	11/11
SUC-B-10	20/100	204/1100	2/2	11/11
SUC-BZ-1	20/100	204/1100	2/2	11/11
SUC-BZ-5	20/100	206/1100	2/2	11/11
SUC-BZ-10	20/100	214/1100	2/2	11/11

6 CONCLUSION AND FUTURE DIRECTIONS

As more wind power is being integrated into the electric power grid, the forecast uncertainty brings operational challenges for the system operators. In this report, different operational strategies for uncertainty management are presented and evaluated. A comprehensive and consistent simulation framework is developed to analyze the performance of different reserve policies and scheduling techniques. The numerical results from the IEEE 118-bus system show that SUC formulations provide a reliable schedule without large increases in operational costs. Moreover, the results indicate that decomposition can help in overcoming the computational obstacles for SUC and can enable the use of a larger scenario set. In contrast, DUC and IUC tend to yield higher system costs as more reserves are being scheduled, but these approaches require much less computational time. The introduction of zonal reserve requirements into DUC improves reliability, but at the expense of higher costs. For DUC and IUC, choosing a proper LB for the forecast uncertainty is important for balancing reliability and system operational cost. The pros and cons of the different operational strategies analyzed in this report are summarized in TABLE 23.

Interesting directions for future work include exploring approaches to optimize the dynamic reserve settings under DUC. Moreover, modeling the ability of wind power to provide reserves should also be considered as a means to obtain a more economical schedule. Testing these operational methods for higher wind penetration levels and for larger scenario sets is also important, as is investigating implications for market clearing and pricing. Finally, the approaches tested in this report should be compared against a wider set of operational strategies.

TABLE 23 Pros and Cons of Different Scheduling Strategies

	Pros	Cons
DUC-DR	Computationally efficient	Conservative; may schedule more units than necessary
	Reduces load shedding compared to no-reserve case	Causes reserve curtailments if the reserve rule is too conservative
DUC-DRZ	Computationally efficient	More conservative and costly than DUC-DR
	More reliable than DUC-DR because of zonal reserve requirements	Causes reserve curtailment if reserve rule is set too high
IUC	Computationally very efficient	May be difficult to find proper LBs for forecast interval
	Reliable schedule with low or no load shedding	Starts more fast units than other formulations
SUC-E	More economic and reliable schedule	Much slower than DUC and IUC
	Starts fewer units	Less scalable with more scenarios
	Captures uncertainty well through stochastic formulation	
SUC-LSF	More economical and reliable schedule	Slower than DUC and IUC
	Starts fewer units	Less scalable with more scenarios
	More computationally efficient than SUC-E	
	Identifies congested transmission lines	
	Captures uncertainty well through stochastic formulation	
SUC-BD	More economic and reliable schedule	Slower than DUC and IUC
	Computationally efficient	Need for more model and parameter tuning than with LSF decomposition
	Better scalability than LSF and SUC-E	
	Captures uncertainty well through stochastic formulation	Bloating master problem if optimality cuts are weak

7 REFERENCES

[1] C. Monteiro, R. Bessa, V. Miranda, A. Botterud, J. Wang and G. Conzelmann, Wind Power Forecasting: State-of-the-Art 2009, Argonne National Laboratory (ANL) Report ANL/DIS-10-1 (2009).

[2] Y. Zhang, J. Wang and X. Wang, "Review on probabilistic forecasting of wind power generation," Renew. Sustain. Energy Rev., vol. 32, pp. 255–270, 2014.

[3] R. J. Bessa, V. Miranda, A. Botterud, Z. Zhou and J. Wang, "Time-adaptive quantile-copula for wind power probabilistic forecasting," Renew. Energy, vol. 40, no. 1, pp. 29–39, 2012.

[4] P. Pinson, "Very short-term probabilistic forecasting of wind power with generalized logit-normal distributions," J. Royal Statist. Soc., Series C, vol. 61, no. 4, pp. 555–576, 2012.

[5] H. A. Nielsen, H. Madsen and T. S. Nielsen, "Using quantile regression to extend an existing wind power forecasting system with probabilistic forecasts," Wind Energy, vol. 9, no. 1–2, pp. 95–108, 2006.

[6] J. Juban, L. Fugon and G. Kariniotakis, "Probabilistic short-term wind power forecasting based on kernel density estimators," Proc. Eur. Wind Energy Conf. (EWEC 07), 2007.

[7] J. Taylor, P. McSharry and R. Buizza, "Wind power density forecasting using ensemble predictions and time series models," IEEE Trans. Energy Convers., vol. 24, no. 3, pp. 775–782, 2009.

[8] Z. Zhou, A. Botterud, J. Wang, R. J. Bessa, H. Keko, J. Sumaili and V. Miranda, "Application of probabilistic wind power forecasting in electricity markets," Wind Energy, vol. 16, pp. 321–338, 2013.

[9] J. Wang, A. Botterud, R. Bessa, H. Keko, L. Carvalho, D. Issicaba, J. Sumaili and V. Miranda, "Wind power forecasting uncertainty and unit commitment," Appl. Energy, vol. 88, no. 11, pp. 4014–4023, 2011.

[10] A. Papavasiliou, S. Oren and R. O'Neill, "Reserve requirements for wind power integration: A scenario-based stochastic programming framework," IEEE Trans. Power Syst., vol. 26, no. 4, pp. 2197–2206, Nov. 2011.

[11] Y. Huang, Q. P. Zheng and J. Wang, "Two-stage stochastic unit commitment model including non-generation resources with conditional value-at-risk constraints," Electr. Power Syst. Res., vol. 116, pp. 427–438, 2014.

[12] Y. Dvorkin, Y. Wang, H. Pandzic and D. S. Kirschen, "Comparison of scenario reduction techniques for the stochastic unit commitment," Proc. 2014 IEEE Power and Energy Soc. Gen. Meeting, pp. 1–5, 2014.

[13] L. Wu, M. Shahidehpour and Z. Li, "Comparison of scenario-based and interval optimization approaches to stochastic SCUC," IEEE Trans. Smart Grid, vol. 27, no. 2, pp. 913–921, 2012.

[14] S. M. Ryan, R. J. B. Wets, D. L. Woodruff, C. Silva-Monroy and J.-P. Watson, "Toward scalable, parallel progressive hedging for stochastic unit commitment," Proc. 2013 IEEE Power and Energy Soc. Gen. Meeting, pp. 1–5, 2013.

[15] C. Uckun, A. Botterud and J. R. Birge, "An improved stochastic unit commitment formulation to accommodate wind uncertainty," IEEE Trans. Power Syst., vol. 31, no. 4, pp. 2507–2517, 2016.

[16] Y. Wang, Q. Xia and C. Kang, "Unit commitment with volatile node injections by using interval optimization," IEEE Trans. Power Syst., vol. 26, no. 3, pp. 1705–1713, 2011.

[17] H. Pandzic, Y. Dvorkin, T. Qiu, Y. Wang and D. S. Kirschen, "Toward cost-efficient and reliable unit commitment under uncertainty," IEEE Trans. Power Syst., vol. 31, no. 2, pp. 970–982, 2016.

[18] C. Liu, Z. Zhou and A. Botterud, "Fuzzy joint energy and reserve auction with high penetration of renewable energy," Working Paper, 2016.

[19] D. Bertsimas, E. Litvinov, X. A. Sun, J. Zhao and T. Zheng, "Adaptive robust optimization for the security constrained unit commitment problem," IEEE Trans. Power Syst., vol. 28, no. 1, pp. 52–63, Feb. 2013.

[20] R. Jiang, J. Wang and Y. Guan, "Robust unit commitment with wind power and pumped storage hydro," IEEE Trans. Power Syst., vol. 27, no. 2, pp. 800–810, May 2012.

[21] D. Pozo and J. Contreras, "A chance-constrained unit commitment with an n-K security criterion and significant wind generation," IEEE Trans. Power Syst., vol. 28, no. 3, pp. 2842–2851, Aug. 2013.

[22] Y. Dvorkin, H. Pandzic, M. Ortega-Vazquez and D. S. Kirschen, "A hybrid stochastic/interval approach to transmission-constrained unit commitment," IEEE Trans. Power Syst., vol. 30, no.2, pp. 621–631, March 2015.

[23] C. Zhao and Y. Guan "Unified stochastic and robust unit commitment," IEEE Trans. Power Syst., vol. 28, no. 3, pp. 3353–3361, Aug. 2013.

[24] Z. Zhou, C. Liu and A. Botterud, Stochastic Methods Applied to Power System Operations with Renewable Energy: A Review, Technical Report No. ANL/ESD-16/14, Argonne National Laboratory, 2016.

[25] Y. Chen, P. Gribik and J. Gardner, "Incorporating post zonal reserve deployment transmission constraints into energy and ancillary services co-optimization," IEEE Trans. Power Syst., vol. 29, no. 2, pp. 537–549, 2014.

[26] N. Growe-Kuska, H. Heitsch and W. Romisch, “Scenario reduction and scenario tree construction for power management problems,” Proc. 2003 IEEE Bologna Power Tech Conference, pp. 1–7, 2003.

[27] J. Sumaili, H. Keko, V. Miranda, Z. Zhou, A. Botterud and J. Wang, "Finding representative wind power scenarios and their probabilities for stochastic models," 16th International Conference on Intelligent System Application to Power Systems (ISAP), 2011, pp. 1–6.

[28] L. Wu, “An improved decomposition framework for accelerating LSF and BD based methods for network-constrained UC problems,” IEEE Trans. Power Syst., vol. 28, no. 4, pp. 3977–3986, Nov. 2013.

[29] H. Bludszuweit, J. A. Dominguez-Navarro and A. Llombart, “Statistical analysis of wind power forecast error,” IEEE Trans. Power Syst., vol. 23, pp. 983–991, 2008.

[30] P. Pinson, G. Papaefthymiou, B. Klöckl, H. A. Nielsen and H. Madsen, “From probabilistic forecasts to statistical scenarios of short-term wind power production,” Wind Energy, vol. 12, no. 1, pp. 51–62, 2009.

[31] G. Papaefthymiou and P. Pinson, “Modeling of spatial dependence in wind power forecast uncertainty,” Proc. 10th Int. Conf. on Probabilistic Methods Applied to Power Systems (PMAPS 2008), pp. 1–9, 2008.

[32] GAMS/SCENRED [online]. Available: http://www.gams.com/dd/docs/solvers/scenred.pdf.

[33] M. Carrion and J. Arroyo, “A computationally efficient mixed-integer linear formulation for the thermal unit commitment problem,” IEEE Trans. Power Syst., vol. 21, no. 3, pp. 1371–1378, 2006.

[34] J. Ostrowski, M. F. Anjos and A. Vannelli, “Tight mixed integer linear programming formulations for the unit commitment problem,” IEEE Trans. Power Syst., vol. 27, no. 1, pp. 39–46, 2012.

[35] G. Morales-Espana, J. M. Latorre and A. Ramos, “Tight and compact MILP formulation for the thermal unit commitment problem,” IEEE Trans. Power Syst., vol. 28, no. 4, pp. 4897–4908, Nov. 2013.

[36] PJM Ancillary Service data [online]. Available: http://www.pjm.com/markets-and-operations/ancillary-services.aspx.

[37] K. Kim and V. M. Zavala, “Large-scale mixed-integer programming algorithms for power generation scheduling” [online]. Available: http://www.mcs.anl.gov/papers/P5382–0715.pdf.

[38] RTO Unit Commitment Test System Staff Report [online]. Available: http://www.ferc.gov/legal/staff-reports/rto-COMMITMENT-TEST.pdf.

[39] Y. Wen, C. Guo, H. Pandzic and D. S. Kirschen, “Enhanced security-constrained unit commitment with emerging utility-scale energy storage,” IEEE Trans. Power Syst., vol. 31, no. 1, pp. 652–662, Jan. 2016.

[40] A. Conejo, E. Castillo, R. Minguez and R. Garcia-Bertrand, Decomposition Techniques in Mathematical Programming, Springer, 2006.

[41] IEEE 118-Bus System [online]. Available: http://motor.ece.iit.edu/data.

[42] Y. Fu, M. Shahidehpour and Z. Li, "Security-constrained unit commitment with AC constraints," IEEE Trans Power Syst., vol. 20, no. 2, pp. 1001–1013, May 2005.

[43] NREL Eastern Wind Dataset [online]. Available: http://www.nrel.gov/electricity /transmission/eastern_wind_methodology.html.

[44] R. Fourer, D. M. Gay and B. W. Kernighan, AMPL: A Modeling Language for Mathematical Programming, Brooks/Cole-Thomson Learning, 2003.

[45] CPLEX 12, IBM ILOG AMPL User's Guide, 2010 [Online]. Available: http://ampl.com/BOOKLETS/amplcplex122userguide.pdf.

[46] FERC, Staff Analysis of Shortage Pricing in RTO and ISO Markets, 2014 [Online]. Available: https://www.ferc.gov/legal/staff-reports/2014/AD14-14-pricing-rto-iso-markets. pdf.

Energy Systems Division
9700 South Cass Avenue, Bldg. 362
Argonne, IL 60439-4854

www.anl.gov

Argonne National Laboratory is a U.S. Department of Energy
laboratory managed by UChicago Argonne, LLC